

Training-Free Motion Customization for Distilled Video Generators with Adaptive Test-Time Distillation

Jintao Rong^{1,2,*} Xin Xie^{2,*} Xinyi Yu¹ Linlin Ou^{1,†} Xinyu Zhang³ Chunhua Shen⁴ Dong Gong^{2,†}
¹Zhejiang University of Technology ²UNSW Sydney ³University of Adelaide ⁴Zhejiang University

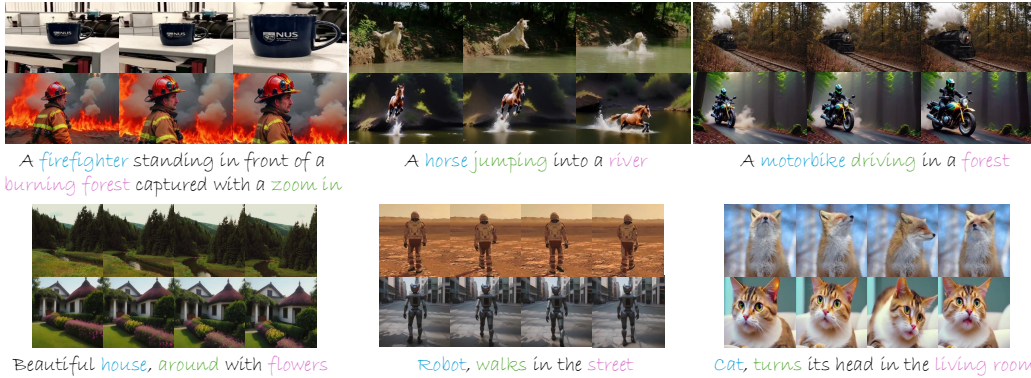


Figure 1: MotionEcho enables training-free, reference-based motion customization for fast distilled video generators (e.g., T2V-TurboV2 [1], top; Animatediff-Lightning [2], bottom) via adaptive, efficient test-time distillation guided by a teacher model. It delivers high-quality motion control across diverse motion types while maintaining efficiency.

Abstract

Distilled video generation models offer fast and efficient synthesis but struggle with motion customization when guided by reference videos, especially under training-free settings. Existing training-free methods, originally designed for standard diffusion models, fail to generalize due to the accelerated generative process and large denoising steps in distilled models. To address this, we propose MotionEcho, a novel training-free test-time distillation framework that enables motion customization by leveraging diffusion teacher forcing. Our approach uses high-quality, slow teacher models to guide the inference of fast student models through endpoint prediction and interpolation. To maintain efficiency, we dynamically allocate computation across timesteps according to guidance needs. Extensive experiments across various distilled video generation models and benchmark datasets demonstrate that our method significantly improves motion fidelity and generation quality while preserving high efficiency. Project page: <https://euminds.github.io/motionecho/>.

1 Introduction

Text-to-video (T2V) diffusion models [3, 4, 5, 6, 7] have significantly advanced video generation, particularly conditional video generation, producing high-quality, temporally coherent videos from

*Equal contribution. The work was done during Jintao Rong’s Research Practicum visit at UNSW.

†Corresponding authors.

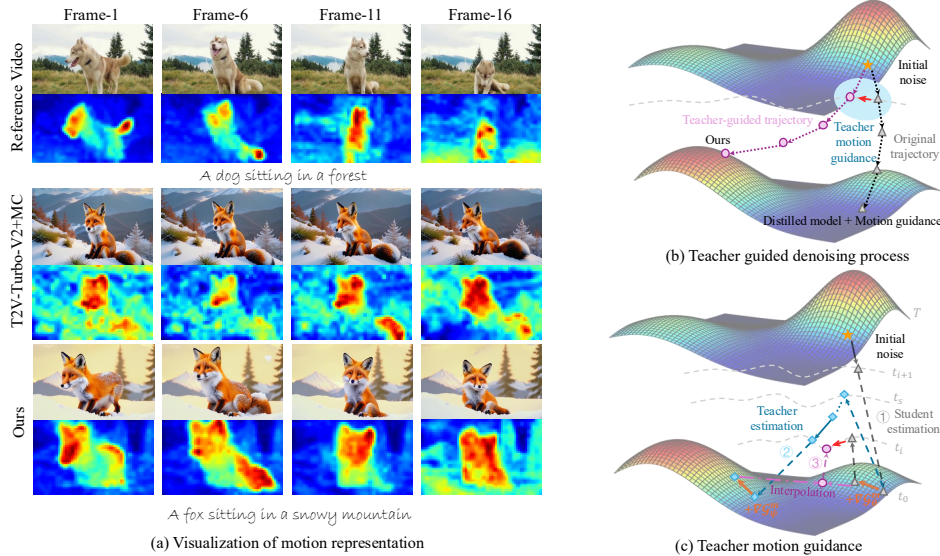


Figure 2: **Overview of MotionEcho.** (a) We visualize motion representations from key temporal attention maps of the denoising U-Net. Our method yields better alignment with the reference, capturing more coherent and consistent motion patterns. (b) Illustration of the test-time distillation process with teacher guidance. Compared to directly combining motion control with the distilled model (gray path), our method more effectively aligns generation with the reference motion (pink path). (c) The student (①) and teacher (②) models perform motion customization via motion loss gradients, with teacher guidance injected through prediction interpolation (③) at sub-interval endpoint.

textual prompts. Given the unique complexity of conditional video generation, recent research has increasingly focused on *motion customization* [8, 9, 10, 11, 12, 13, 14, 15, 16], enabling generated videos to mimic motion patterns from *reference videos* as a condition while synthesizing novel content. Motion customization in T2V can be achieved through *training-based* methods [8, 9, 10, 11, 13, 12], which integrate motion information by applying LoRA[17] or full model fine-tuning to embed motion representations directly into the model. To support more flexible and accessible motion customization across different T2V models without extensive training process, *training-free* methods [14, 15, 16] incorporate motion patterns via *inference-time* optimization and calculations with regularization-based guidance, without prior model training. Although training-free methods avoid model training, they typically involve additional inference-time procedures aligned with the inherently iterative nature of diffusion models, leading to increased computational overhead.

Despite producing high-quality results, the iterative sampling process of diffusion models is inherently slow, limiting T2V’s real-world applications. To accelerate inference, recent studies [18, 7, 1, 2] leverage consistency distillation [19, 20] to distill an efficient video consistency model (VCM) from a *teacher* T2V model, enabling high-quality video generation in just 4–8 inference steps [7]. Against this background, we pose the following question: *Can we enable training-free motion customization on a distilled, fast T2V model, achieving high-quality motion control while maintaining inference efficiency?* To explore this, we conduct preliminary studies and analyses (Fig.2) by directly applying existing training-free motion customization methods (e.g., MotionClone [14]) to distilled, fast T2V models (e.g., T2V-Turbo-V2 [1]). The results reveal notable issues such as temporal inconsistency, motion artifacts, and misinterpreted motion, e.g., the fox’s head fails to follow the reference motion of a dog’s head. We attribute this degradation to two main factors: (1) Distilled models collapse multiple denoising steps into one and have only few steps, making the progressive interventions used in training-free methods coarse and less effective. (2) The denoising behavior of distilled models (trained to compress behavior) differs significantly from that of teacher models trained with dense timesteps, rendering the original motion guidance strategies incompatible. Moreover, consistency models bypass explicit noise control, and training-free motion customization operations are not incorporated during distillation, limiting the effectiveness of inversion-based techniques [14].

In this work, we aim to achieve fast and temporally consistent motion customization on the fast distilled video generators. We introduce `MotionEcho`, a novel training-free framework for inference-time motion customization on distilled fast T2V models. It efficiently incorporates adaptive test-time distillation guided by a teacher model to enable high-quality motion control. To address quality degradation caused by applying motion guidance directly to distilled models, we leverage a diffusion-based teacher model with motion control to provide fine-grained guidance to the fast student. This guidance is applied via endpoint prediction and interpolation during the student’s reverse steps, serving as an *echo* of the teacher model. To maintain efficiency, this test-time distillation is applied step-wise and selectively during the student’s inference. Additionally, we propose an adaptive acceleration strategy that dynamically decides when teacher supervision is necessary and adjusts the number of optimization steps accordingly at each denoising step, balancing quality and efficiency.

The main contributions are summarized as:

- We reveal the limitations of directly applying existing training-free motion customization methods to fast distilled T2V models and propose `MotionEcho`, a novel training-free framework that introduces test-time motion customization via teacher-guided distillation during inference.
- We propose an adaptive acceleration strategy that dynamically schedules teacher guidance and adjusts the optimization budget per denoising step, effectively balancing motion quality and inference efficiency.
- We validate our `MotionEcho` on diverse pre-trained distilled video diffusion models, *e.g.*, T2V-Turbo-V2, AnimateDiff-Lightning, *etc.* Experiments show that our method consistently outperforms state-of-the-art training-based and training-free motion customization approaches across multiple metrics, demonstrating superior efficiency and effectiveness.

2 Related Work

2.1 Text-to-Video Diffusion Models

With the advent of diffusion models [21, 22, 23], remarkable advancements in content creation have been witnessed in the text-to-image field [24, 25, 26, 27, 28, 29, 30, 31]. Following this success, recent text-to-video diffusion models, including SORA [6], GEN-3 Alpha [32], and Veo [5], have achieved high-quality video generation but remain unavailable to the public. To break the limitation, the seminal work VDM [3] leverage a 3D UNet [33], factorized over space and time, for unconditional video generation. Subsequently, Imagen Video [34] and Make-a-Video [35] adopt cascade frameworks to enable high-resolution text-conditioned video generation in pixel space. To reduce the computational cost, LVDM [36], VideoLDM [37], and MagicVideo [38] extend diffusion models to a 3D latent space, facilitating training on large-scale video datasets [39, 40]. Rather than training from scratch, AnimateDiff [41] trains a domain adapter for quality enhancement and a temporal module for motion prior learning via lightweight LoRAs [17]. VideoCrafter1 [4] upgrades the SD model [28] by incorporating temporal attention layers into the UNet for temporal consistency. VideoCrafter2 [42] further disentangles low-quality videos for motion learning and high-quality images for appearance learning. Due to the iterative nature of diffusion model [22], T2V-Turbo [7] and T2V-Turbo-V2 [1] adopt the consistency models [19] to distill from VideoCrafter2 [42], thereby accelerating the sampling process. AnimateDiff-Lightning [2] achieves few-step video generation by progressive adversarial diffusion distillation.

2.2 Video Motion Customization

Motion customization aim to enable the generated videos to follow specific motion patterns from reference videos while remaining semantically aligned with the given textual descriptions. Pioneering work Tune-A-Video [43] introduces one-shot video generation by tuning SD [28] on a single reference video. ControlVideo [12] and Text2Video-Zero [16] inherit priors from ControlNet [44] and leverage cross-frame interactions to enable zero-shot controllable video synthesis. Furthermore, Control-A-Video [13] employ trainable motion layers to UNet and ControlNet [44] for temporal modeling, achieving motion control conditioned on depth, sketch, or motion information from reference videos. Despite achieving high-quality video customization, these methods still suffer from motion misalignment. To address this issue, existing motion-specific tuning methods, such as VMC [8],

MotionDirector [9] and MotionInversion [10], are designed to decouple the learning of appearance and motion, enabling the generalization of distinct motion patterns to diverse textual prompts and scenes. Additionally, DMT [15] and MotionClone [14] employ training-free strategies, extracting motion priors from the latent representations of reference videos and constructing an energy function to guide motion customization during inference. Zhang *et al.* [45] propose a motion consistency loss combined with inverted reference noise to enhance temporal coherence and motion accuracy.

3 Preliminaries

Video Diffusion Models. Video diffusion models [22, 28] generate videos by progressively denoising random noise through a learned reverse diffusion process. Given an input video x , a pre-trained encoder \mathcal{E} maps it into the latent space $z_0 = \mathcal{E}(x)$, which is gradually corrupted into $z_t = \sqrt{\bar{\alpha}_t}z_0 + \sqrt{1 - \bar{\alpha}_t}\epsilon_t$, where $\epsilon_t \sim \mathcal{N}(0, \mathbf{I})$ represents Gaussian noise and $\bar{\alpha}_t$ is a hyperparameter for controlling the diffusion process. To capture the data distribution, a neural network ϵ_θ is trained to estimate the added noise from noise input z_t , which is formulated as follows:

$$\min_{\theta} \mathbb{E}_{\mathcal{E}(x), \epsilon_t \sim \mathcal{N}(0, \mathbf{I}), t \sim \mathcal{U}(1, T)} \left[\|\epsilon_t - \epsilon_\theta(z_t, c, t)\|_2^2 \right], \quad (1)$$

where c is the condition such as the textual prompt. During inference, the sampling process begins with a standard Gaussian noise. To enhance the controllability, we typically introduce classifier-free guidance [46] or additional customized energy function $\mathcal{G}(z_t, t)$ [47, 48] during sampling, *i.e.*,

$$\hat{\epsilon}_\theta = \epsilon_\theta(z_t, c, t) + \omega(\epsilon_\theta(z_t, c, t) - \epsilon_\theta(z_t, \phi, t)) - \eta \nabla_{z_t} \mathcal{G}(z_t, t), \quad (2)$$

where ω and η are scaling factors that determine the strength of guidance.

Motion Customization in Video Generation. Despite success of high-quality video generation, text-to-video diffusion models struggle to reflect user-intended motion solely from textual prompts. This limitation has sparked growing interest in motion customization, aiming to generate videos that replicate the reference motion. While training-based approaches [9, 10, 43, 13, 11, 12] learn motion representations from reference videos through fine-tuning or LoRA-based model adaptation [17], training-free methods [15, 14, 45] injecting motion priors at inference time, optimizing the sampling process via motion-conditioned guidance. Both paradigms share a common objective: minimizing the discrepancy between the motion representations of the generated and reference videos $\mathbb{E}_{z_0, z_t^{\text{ref}}, t, \epsilon_t} \left[\|\mathcal{M}(z_t^{\text{ref}}) - \mathcal{M}(z_t^\theta)\|_2^2 \right]$, where $\mathcal{M}(\cdot)$ is a motion feature extractor for noisy latent videos and z_t^{ref} is the noisy reference latent obtained via DDIM inversion [21].

Distillation for Accelerated Video Diffusion Models. The inherently iterative nature of video diffusion models results in slow inference and substantial computational overhead. To alleviate this issue, recent efforts [2, 49, 7, 1] leverage knowledge distillation [50] to compress the generation process by training a compact student model ϵ_ψ to approximate the denoising trajectories of the teacher ϵ_θ under a coarser timestep schedule $\mathcal{U}_\psi(1, T)$. This distillation process enables high-fidelity video synthesis with drastically reduced inference steps: $\min_{\psi} \mathbb{E}_{z_0, c, t \sim \mathcal{U}_\psi(1, T)} \left[\|\epsilon_\psi(z_t, c, t) - \epsilon_\theta(z_t, c, t)\|_2^2 \right]$.

4 Methodology

Overview. We propose a training-free framework for motion customization in fast distilled T2V models by leveraging test-time distillation with teacher guidance. We begin by exploring the direct application of existing training-free motion customization methods to distilled models, but observe significant visual artifacts and temporal inconsistencies due to coarse denoising and mismatched behavior. To address this, we introduce a fine-grained teacher model with motion customization to guide the student via score distillation during inference. To maintain the efficiency, we develop an adaptive acceleration strategy that selectively activates teacher guidance and dynamically adjusts its denoising steps. The whole pipeline of proposed method is demonstrated in Fig. 3.

4.1 Test-time Motion Customization for Distilled Video Generators

To improve the efficiency of motion customization during test-time inference, we explore an intuitive solution that directly integrates motion control [14, 9] into the sampling process of the distilled video

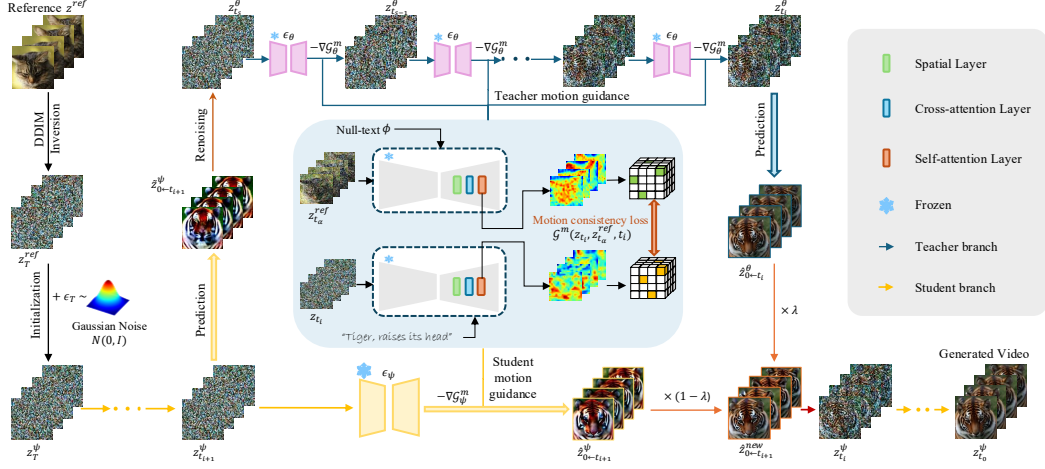


Figure 3: **Pipeline of MotionEcho.** Given a reference video, motion priors are extracted to initialize the student model with a motion-preserving noisy latent. During inference, the teacher (top) and student (bottom) models perform motion customization using motion loss gradients. Teacher guidance is applied via prediction interpolation at sub-interval endpoints. The student then generates the final video in a few steps with high motion fidelity.

diffusion model ϵ_ψ . This solution retains the efficiency of the distilled student model while injecting motion representations without any training. For each large denoising step from t_{i+1} to t_i in the distilled model, the predicted noise is modified as:

$$\hat{\epsilon}_\psi(z_{t_{i+1}}^\psi, c, t_{i+1}) = \tilde{\epsilon}_\psi(z_{t_{i+1}}^\psi, c, t_{i+1}) - \eta \nabla_{z_{t_{i+1}}^\psi} \mathcal{G}^m(z_{t_{i+1}}^\psi, z_{t_\alpha}^{ref}, t_{i+1}), \quad (3)$$

where $\tilde{\epsilon}_\psi(z_{t_{i+1}}^\psi, c, t_{i+1}) = (1 + \omega_\psi)\epsilon_\psi(z_{t_{i+1}}^\psi, c, t_{i+1}) - \omega_\psi\epsilon_\psi(z_{t_{i+1}}^\psi, \phi, t_{i+1})$ denotes classifier-free guidance [46]. Following MotionClone [14], $\mathcal{G}^m(z_{t_{i+1}}^\psi, z_{t_\alpha}^{ref}, t_{i+1}) = \|M_{t_\alpha}^{ref} \cdot (\mathcal{A}(z_{t_\alpha}^{ref}) - \mathcal{A}(z_{t_{i+1}}^\psi))\|_2^2$ is the motion loss function, where $\mathcal{A}(\cdot)$ represents the temporal attention map and $M_{t_\alpha}^{ref}$ is a temporal mask derived from $\mathcal{A}(z_{t_\alpha}^{ref})$ at a fixed timestep t_α to enforce focused motion supervision and we only apply motion guidance during the initial τ percent of the sampling process. Then, we update $z_{t_i}^\psi$ by renoising the predicted clean latent:

$$z_{t_i}^\psi = \sqrt{\bar{\alpha}_{t_i}} \hat{z}_{0 \leftarrow t_{i+1}}^\psi + \sqrt{1 - \bar{\alpha}_{t_i}} \epsilon_{t_i}, \quad (4)$$

where $\hat{z}_{0 \leftarrow t_{i+1}}^\psi = \frac{z_{t_{i+1}}^\psi - \sqrt{1 - \bar{\alpha}_{t_{i+1}}} \hat{\epsilon}_\psi(z_{t_{i+1}}^\psi, c, t_{i+1})}{\sqrt{\bar{\alpha}_{t_{i+1}}}}$ is the one-step prediction result. With only a few denoising steps, the distilled model efficiently achieve motion customization. However, we observe that visual degradation and temporal inconsistency appear in the generated videos, especially in scenarios with complex object layouts or rapid movements, as shown in Fig. 7. We argue this degradation attributed to the inherent limitations of the distilled model. First, the large denoising step size leads to insufficient motion transfer. Second, the distilled model merely mimics the denoised output without possessing true denoising capabilities, resulting in a mismatch with motion guidance. These issues collectively suggest that directly applying motion customization to the distilled model is suboptimal and ultimately ineffective for high-quality motion control.

4.2 Test-time Distillation with Teacher Motion Guidance

To support efficient and effective motion customization at inference time, we introduce a test-time distillation framework that leverages a fine-grained teacher T2V diffusion model ϵ_θ to guide a distilled student model ϵ_ψ . We first apply motion customization to the teacher model, aligned with the reference motion. Subsequently, the customized teacher provide guidance by refine the student’s one-step predictions, effectively transferring motion without requiring retraining.

Motion Customization for Teacher Model. Different from Sec. 4.1, the motion customization process in the distilled model begins with a reference-aware noise initialization. Following previous studies [51, 52, 15], we align the temporal dynamics priors of the reference video by blending the inverted reference latent z_T^{ref} with random noise ϵ_T , forming a hybrid noise $z_T^\psi = \sqrt{k} \cdot z_T^{\text{ref}} + \sqrt{1-k} \cdot \epsilon_T$, where k controls the trade-off between motion preservation and content generalization. To maintain the spatial consistency and bridge the mismatch between the student’s coarse and the teacher’s fine-grained timestep schedules, we renoise the student’s predicted clean latent without motion guidance $\hat{z}_{0 \leftarrow t_{i+1}}^\psi = \frac{z_{t_{i+1}}^\psi - \sqrt{1-\bar{\alpha}_{t_{i+1}}} \bar{\epsilon}_\psi(z_{t_{i+1}}^\psi, c, t_{i+1})}{\sqrt{\bar{\alpha}_{t_{i+1}}}}$ to an intermediate timestep $t_s \in [t_{i+1}, t_i]$ on the teacher’s trajectory. Then, the teacher model follow Eq.(3) and Eq.(4) to perform iterative motion customization: $z_{t_s-1}^\theta \leftarrow z_{t_s}^\theta + \bar{\epsilon}_\theta(z_{t_s}^\theta, c, t_s) - \eta \nabla_{z_{t_s}^\theta} \mathcal{G}^m(z_{t_s}^\theta, z_{t_s}^{\text{ref}}, t_s)$.

Test-time Distillation of Teacher Motion. To preserve the efficiency of the distilled model, we utilize the score distillation sampling loss $\ell_{\text{distill}}(z; \psi, \theta) = \|\hat{z}_{0 \leftarrow t_{i+1}}^\psi - \hat{z}_{0 \leftarrow t_i}^\theta\|_2^2$ to transfer knowledge from teacher to student. We thus refine Eq.(4) to update $z_{t_i}^\psi$ as follow:

$$z_{t_i}^\psi = \sqrt{\bar{\alpha}_{t_i}} (\hat{z}_{0 \leftarrow t_{i+1}}^\psi - \lambda \nabla_{\hat{z}_{0 \leftarrow t_{i+1}}^\psi} \ell_{\text{distill}}) + \sqrt{1 - \bar{\alpha}_{t_i}} \epsilon_{t_i} = \sqrt{\bar{\alpha}_{t_i}} \hat{z}_{0 \leftarrow t_{i+1}}^{\text{new}} + \sqrt{1 - \bar{\alpha}_{t_i}} \epsilon_{t_i}, \quad (5)$$

where $\hat{z}_{0 \leftarrow t_{i+1}}^{\text{new}} = (1 - \lambda) \hat{z}_{0 \leftarrow t_{i+1}}^\psi + \lambda \hat{z}_{0 \leftarrow t_i}^\theta$ and λ controls the strength of teacher guidance.

4.3 Adaptive Acceleration Strategy for Efficiency.

A straightforward approach to ensure accurate motion transfer is to apply teacher supervision at every timestep within the initial τ percent of the student model’s sampling process. However, this leads to two critical issues. First, since different timesteps exhibit varying denoising capabilities, applying teacher guidance at every student step is unnecessary and may become counterproductive. Second, the iterative denoising process in the teacher model is costly, as each timestep interval in the student model spans a relatively long temporal range. To optimize budget utilization, we design an adaptive acceleration strategy composed of two core components as detailed below.

Step-wise Guidance Activation. Due to the large denoising intervals taken by the student model, the decision to apply teacher guidance at each step becomes critical, which significantly affects the effectiveness of motion transfer. To make this decision more robust, we evaluate the necessity of distillation by computing the average motion loss over a moving window of previous steps, $\mathcal{G}_{t_i}^\psi = \frac{1}{W} \sum_{j=0}^{W-1} \mathcal{G}^m(z_{t_{i+j}}^\psi, z_{t_i}^{\text{ref}}, t_{i+j})$, where t_i denotes the current timestep and W is the window size. If the average motion loss $\mathcal{G}_{t_i}^\psi$ exceeds a predefined threshold δ_1 , we activate teacher guidance for this step.

Dynamic Truncation. Once guidance is triggered, we further optimize the internal denoising steps performed by the teacher model. Instead of using a fixed number of denoising steps, we conduct a dynamic truncation based on the smoothness of the motion loss. Specifically, during the interval from t_s to t_i , we monitor the motion loss $\mathcal{G}^m(z_{t_s}^\theta, z_{t_s}^{\text{ref}}, t_s)$. If the loss falls below a confidence threshold δ_2 , we terminate the motion transfer early and directly de-noise the current latent to the latent of t_i . Additionally, to prevent excessive computation when the loss remains high, we impose an upper limit N_{max} on the number of denoising iterations.

5 Experiments

In this section, we present the experimental results conducted on a wide range of distilled video generators to verify the effectiveness of our method. We validate the performance of our method through comparing with existing state-of-the-art motion customization approaches. We delve deeper into the role of each component in our test-time distillation framework, supported by ablation studies.

5.1 Experimental Setting

Implementation Details. Without requiring additional training, our method can be seamlessly integrated with various generative video diffusion models. To facilitate discussion, we denote

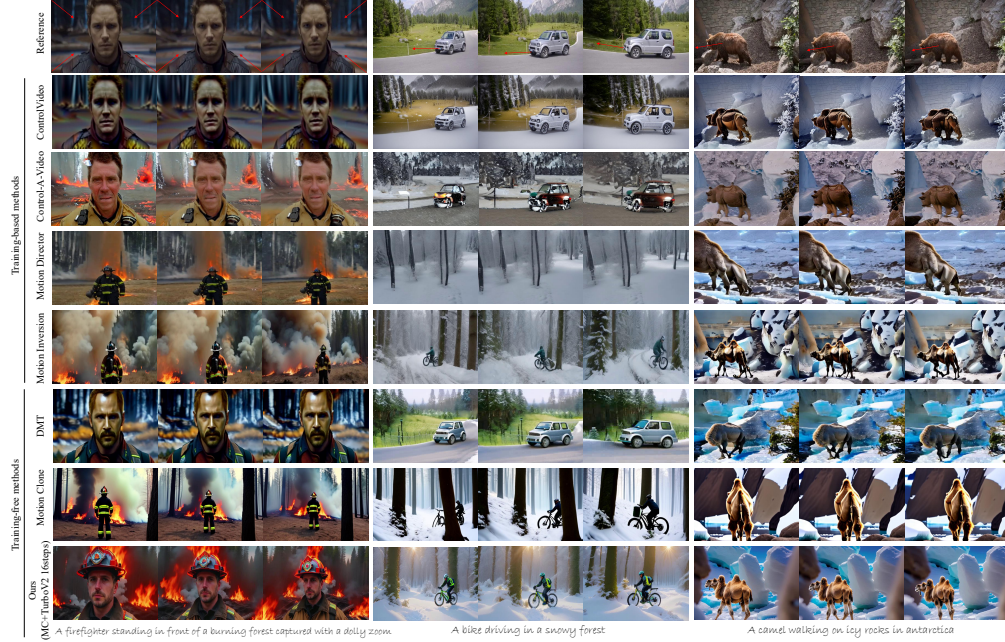


Figure 4: **Qualitative comparisons on VideoCrafter2-based methods.** Our method enables unified object, camera, and hybrid motion transfer with high motion fidelity and low inference time.

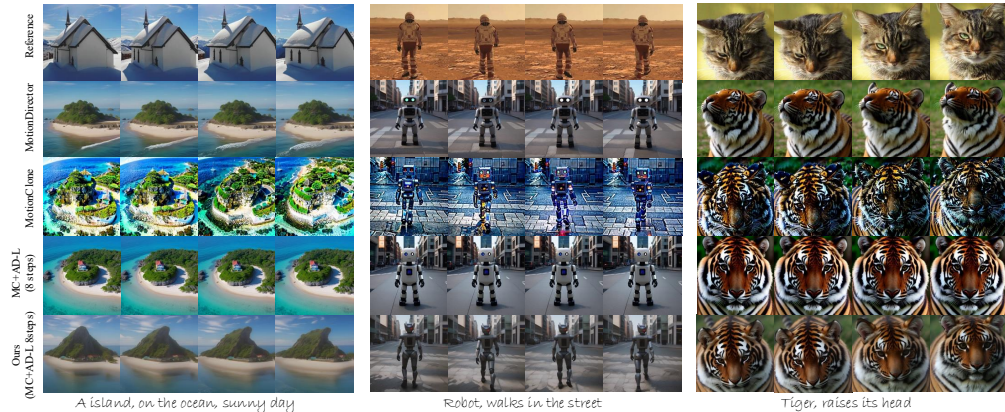


Figure 5: **Qualitative comparisons on AnimateDiff-based methods.** Our methods enables the effective transfer of object and camera motion.

the models by their abbreviations in parentheses). During inference, VideoCrafter2 [42] (VC2) is employed as the teacher model to provide guidance for the distilled model, T2V-Turbo-V2 [1] (TurboV2). To further demonstrate the scalability of our method, MotionEcho is generalized to the distilled model AnimateDiff-Lightning [2] (AD-L), using AnimateDiff [41] (AD) as the teacher model. Additionally, we use MotionClone [14] (MC) and MotionDirector (MD) [9] to align reference motion for the teacher and student models. For TurboV2, the step-wise activation threshold δ_1 ranges from 380 to 420 according motion types, with a dynamic truncation threshold δ_2 of 380. For AD-L, δ_1 ranges from 360 to 400, and δ_2 is set to 360. All our experiments are conducted using a NVIDIA A100-40G GPU.

Datasets. We evaluate our method on two distinct benchmarks. For methods based on TurboV2 and VC2, we keep consistent with prior works [15, 10], using source videos obtained from DAVIS dataset [53], WebVID dataset [54], and online video resources. We refer the combined validation dataset as TurboBench, consisting of 66 video-edit text pairs derived from 22 unique videos, which

Table 1: Quantitative comparison of VideoCrafter2-based methods on TurboBench.

Method	Temporal Consistency (↑)	Text Alignment (↑)	Motion Fidelity (↑)	FID (↓)	Inference Time Cost (↓)	Training Time Cost (↓)
ControlVideo [12]	0.9420	0.251	0.964	379.37	80s	450s
Control-A-Video [13]	0.925	0.256	0.858	383.95	20s	hours
MotionDirector [9]	0.922	0.329	0.851	373.21	10s	280s
MotionInversion [10]	0.951	0.321	0.885	351.72	32s	489s
DMT [15]	0.961	0.259	0.909	367.18	316s	-
MotionClone [14]	0.978	0.335	0.876	369.49	114s	-
Ours (MC+TurboV2 16 steps)	0.976	0.348	0.933	322.97	13s	-
Ours (MC+TurboV2 8 steps)	0.967	0.338	0.931	335.65	9s	-
Ours (MC+TurboV2 4 steps)	0.956	0.323	0.927	347.91	6s	-

Table 2: Quantitative comparison of AnimateDiff-based methods on AnimateBench.

Method	Temporal Consistency (↑)	Text Alignment (↑)	Motion Fidelity (↑)	FID (↓)	Inference Time Cost (↓)	Training Time Cost (↓)
MotionDirector [9]	0.961	0.304	0.833	378.31	18s	451s
MotionClone [14]	0.957	0.321	0.849	367.07	203s	-
MC+AD-L (8steps) [14]	0.974	0.322	0.648	357.15	7s	-
Ours (MC+AD-L 8 steps)	0.981	0.327	0.868	336.03	24s	-
Ours (MC+AD-L 4 steps)	0.973	0.319	0.854	348.99	17s	-

comprehensively spans diverse real-world scenarios, encompassing multiple object categories, varied scene configurations, and rich motion patterns ranging from simple translational movements to complex non-rigid deformations. For methods based on AD and AD-L, we make a thorough analysis on 15 real videos from MotionClone [14], comprising 7 videos with camera motion and 8 videos for object motion, hereafter referred to as AnimateBench.

Metrics. To ensure a comprehensive assessment, we perform an evaluation from multiple perspectives. (1) **Text Alignment:** The metric measures how well the generated video content corresponds to the input text prompt by calculating the average cosine similarity between the embeddings of all video frames and the text embeddings, using the CLIP model [55]. (2) **Temporal Consistency:** The metric evaluates the visual smoothness and coherence of generated videos. We compute cosine similarities between the CLIP image embeddings [55] across frames and aggregate results into a stability score, which reflects flicker artifacts and semantic discontinuities while allowing motion-driven appearance changes. (3) **Motion Fidelity:** We assess the effectiveness of motion transfer using the Motion Fidelity Score [15]. The metric relies on motion trajectories extracted via Co-Tracker [56] and computes the geometric consistency between the motion patterns in the source and generated videos. (4) **Fréchet Inception Distance (FID):** We construct a reference image set from selected source videos and evaluate the quality of our generated videos using FID [57]. (5) **Time Cost:** This measures the total time required to complete motion transfer from a reference video. To ensure a fair comparison, additional fine-tuning or optimization steps should be taken into account.

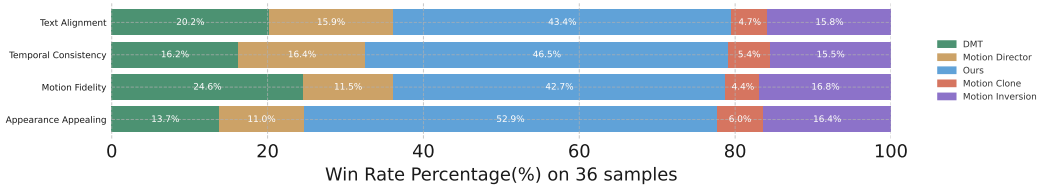


Figure 6: User study results.

5.2 Comparison with Existing Methods

To verify the effectiveness of our approach, we compare MotionEcho with training-based and training-free models. The former comprises ControlVideo [12], Control-A-Video [13], MotionDirector [9], MotionInversion [10]. The latter includes MotionClone [14] and DMT [15].

Quantitative Analysis. To objectively evaluate the performance of our method, we conduct quantitative comparisons on two benchmarks using different base models. As shown in Tab. 1, our method (MC+TurboV2 16 steps) achieves the best performance across text alignment, motion fidelity, and FID score, while maintaining competitive temporal consistency within just 13 seconds. Compared

Table 3: Ablation study results.

Method	Temporal Consistency (\uparrow)	Text Alignment (\uparrow)	Motion Fidelity (\uparrow)	Inference Time Cost (\downarrow)
MD+TurboV2 (16 steps)	0.965	0.327	0.806	4s
MC+TurboV2 (16 steps)	0.967	0.324	0.833	7s
T2V-Turbo-V2(16 steps)	0.973	0.348	0.562	4s
+Motion guidance (MotionClone)	0.967	0.324	0.833	7s
+Inverted reference noise	0.968	0.329	0.896	7s
+Teacher guidance (MC+VideoCrafter2)	0.965	0.336	0.912	20s
+Adaptive acceleration strategy (Ours)	0.976	0.348	0.933	13s



Figure 7: Visualization of the ablation study results.

to prior methods, Control-A-Video [13] and MotionDirector [9] show similar or higher inference times but significantly lower scores in key quality metrics and require costly training. Nevertheless, our method can reduce the inference steps while remaining highly competitive. With only 8 steps, it outperforms most baselines across all metrics in just 9 seconds. Even at 4 steps, it achieves a FID of 347.91 and maintains solid temporal consistency, reducing inference time to only 6 seconds. Additionally, we apply our method into other distilled video models (*e.g.* AD-L) and the results in Tab. 2 further verify the effectiveness, superiority and flexibility of our method.

Qualitative Evaluation. We separately evaluate our method through qualitative comparisons against baselines based on VideoCrafter2 and AnimateDiff frameworks. In Figure 4, compared to over-smoothing and structural collapse observed in prior motion customization models, our method preserves spatial details while achieving high motion fidelity, particularly under challenging scenarios such as dolly zooms, snowy forests, and complex multi-object scenes. In Figure 5, our method based on AD-L shows better motion alignment and temporal consistency than both MotionClone [14] and Motion Director [9]. For example, our method handles subtle motions (*e.g.*, head turning) and large camera movements (*e.g.*, rotating island) more effectively, with fewer artifacts and less drift. These visual results further validate the effectiveness of our method in achieving unified and high-fidelity motion transfer across different distilled video generators, while maintaining efficient inference.

User Study. We perform a user study to objectively assess our method (MC+TurboV2 16 steps) in comparison with VideoCrafter2-based methods including DMT [15], MotionClone [14], MotionInversion [10], Motion Director [9]. We randomly sample 36 video-edit text pairs from TurboBench dataset and synthesize motion videos with aforementioned methods. We invite 50 participants and request them to compare all generated videos from four different aspects: Q1 Text Alignment (Which video better fits the target text description?), Q2 Temporal Consistency (Which video is more consistent across frames?), Q3 Motion Fidelity (Which video better reproduces the motion pattern in the reference?), Q4 Appearance Appealing (Which video is more visually appealing?). Fig. 6 shows the approval percentage of each method in four aspects, which demonstrates our method outperforms the previous motion customization models on human feedbacks.

5.3 Ablation Study

To assess the effect of each component in our test-time distillation framework, we perform ablation studies based on TurboV2 and TurboBench dataset. As shown in Tab. 3 and Fig. 7, directly applying

motion guidance (e.g., MotionClone [14] and MotionDirector [9]) into the distilled model enhances motion fidelity but slightly degrades temporal consistency and text alignment. The visual results (the second row) show unstable motion and poor tracking of the reference. Incorporating the inverted reference noise helps improve motion fidelity by aligning the dynamics priors and reducing contextual bias, but the generated motion remains imprecise. Then, we add test-time guidance from a fine-grained teacher (e.g. VideoCrafter2 [42]) with motion customization significantly boosts both text alignment and motion fidelity, at the cost of increased inference time. To preserve efficiency, our proposed adaptive acceleration strategy effectively reduces the computational cost while maintaining strong performance across all metrics, achieving the best trade-off between quality and efficiency.

6 Conclusion

We propose a training-free framework for efficient motion customization in fast distilled text-to-video diffusion models. Existing training-free methods struggle with coarse denoising and mismatched sampling in distilled models. To address this, we introduce test-time distillation using a motion-controllable teacher to guide the student via score-based supervision. An adaptive acceleration strategy further balances motion fidelity and efficiency. Experiments show our method significantly improves motion consistency and visual quality while maintaining fast generation. **Limitations and future work.** Similar to most training-free methods, the proposed approach lacks a looped quality-checking mechanism during inference. In future work, we plan to investigate strategies for assessing and ensuring output quality at test time. We also aim to extend the method’s applicability to a broader range of base models and explore further opportunities for acceleration.

References

- [1] Jiachen Li, Qian Long, Jian Zheng, Xiaofeng Gao, Robinson Piramuthu, Wenhui Chen, and William Yang Wang. T2v-turbo-v2: Enhancing video generation model post-training through data, reward, and conditional guidance design. *arXiv preprint arXiv:2410.05677*, 2024.
- [2] Shanchuan Lin and Xiao Yang. Animatediff-lightning: Cross-model diffusion distillation. *arXiv preprint arXiv:2403.12706*, 2024.
- [3] Jonathan Ho, Tim Salimans, Alexey Gritsenko, William Chan, Mohammad Norouzi, and David J Fleet. Video diffusion models. *Advances in Neural Information Processing Systems*, 35:8633–8646, 2022.
- [4] Haoxin Chen, Menghan Xia, Yingqing He, Yong Zhang, Xiaodong Cun, Shaoshu Yang, Jinbo Xing, Yaofang Liu, Qifeng Chen, Xintao Wang, et al. Videocrafter1: Open diffusion models for high-quality video generation. *arXiv preprint arXiv:2310.19512*, 2023.
- [5] Abhishek Sharma, Adams Yu, Ali Razavi, Andeep Toor, Andrew Pierson, Ankush Gupta, Austin Waters, Aäron van den Oord, Daniel Tanis, Dumitru Erhan, Eric Lau, Eleni Shaw, Gabe Barth-Maron, Greg Shaw, Han Zhang, Henna Nandwani, Hernan Moraldo, Hyunjik Kim, Irina Blok, Jakob Bauer, Jeff Donahue, Junyoung Chung, Kory Mathewson, Kurtis David, Lasse Espeholt, Marc van Zee, Matt McGill, Medhini Narasimhan, Miaosen Wang, Mikołaj Bińkowski, Mohammad Babaeizadeh, Mohammad Taghi Saffar, Nando de Freitas, Nick Pezzotti, Pieter-Jan Kindermans, Poorva Rane, Rachel Hornung, Robert Riachi, Ruben Villegas, Rui Qian, Sander Dieleman, Serena Zhang, Serkan Cabi, Shixin Luo, Shlomi Fruchter, Signe Nørly, Srivatsan Srinivasan, Tobias Pfaff, Tom Hume, Vikas Verma, Weizhe Hua, William Zhu, Xinchun Yan, Xinyu Wang, Yelin Kim, Yuqing Du, and Yutian Chen. Veo. *Placeholder Journal*, 2024.
- [6] OpenAI. Video generation models as world simulators, 2024. Sora technical report.
- [7] Jiachen Li, Weixi Feng, Tsu-Jui Fu, Xinyi Wang, Sugato Basu, Wenhui Chen, and William Yang Wang. T2v-turbo: Breaking the quality bottleneck of video consistency model with mixed reward feedback. *arXiv preprint arXiv:2405.18750*, 2024.
- [8] Hyeonho Jeong, Geon Yeong Park, and Jong Chul Ye. Vmc: Video motion customization using temporal adaption for text-to-video diffusion models. In *Proceedings of the IEEE/CVF Conference on Computer Vision and Pattern Recognition*, pages 9212–9221, 2024.

- [9] Rui Zhao, Yuchao Gu, Jay Zhangjie Wu, David Junhao Zhang, Jia-Wei Liu, Weijia Wu, Jussi Keppo, and Mike Zheng Shou. Motiondirector: Motion customization of text-to-video diffusion models. In *European Conference on Computer Vision*, pages 273–290. Springer, 2024.
- [10] Luozhou Wang, Ziyang Mai, Guibao Shen, Yixun Liang, Xin Tao, Pengfei Wan, Di Zhang, Yijun Li, and Yingcong Chen. Motion inversion for video customization. *arXiv preprint arXiv:2403.20193*, 2024.
- [11] Yabo Zhang, Yuxiang Wei, Dongsheng Jiang, Xiaopeng Zhang, Wangmeng Zuo, and Qi Tian. Controlvideo: Training-free controllable text-to-video generation. *arXiv preprint arXiv:2305.13077*, 2023.
- [12] Min Zhao, Rongzhen Wang, Fan Bao, Chongxuan Li, and Jun Zhu. Controlvideo: conditional control for one-shot text-driven video editing and beyond. *Science China Information Sciences*, 68(3):132107, 2025.
- [13] Weifeng Chen, Yatai Ji, Jie Wu, Hefeng Wu, Pan Xie, Jiashi Li, Xin Xia, Xuefeng Xiao, and Liang Lin. Control-a-video: Controllable text-to-video diffusion models with motion prior and reward feedback learning. *arXiv preprint arXiv:2305.13840*, 2023.
- [14] Pengyang Ling, Jiazi Bu, Pan Zhang, Xiaoyi Dong, Yuhang Zang, Tong Wu, Huaian Chen, Jiaqi Wang, and Yi Jin. Motionclone: Training-free motion cloning for controllable video generation. *arXiv preprint arXiv:2406.05338*, 2024.
- [15] Danah Yatim, Rafail Fridman, Omer Bar-Tal, Yoni Kasten, and Tali Dekel. Space-time diffusion features for zero-shot text-driven motion transfer. In *Proceedings of the IEEE/CVF Conference on Computer Vision and Pattern Recognition*, pages 8466–8476, 2024.
- [16] Levon Khachatryan, Andranik Movsisyan, Vahram Tadevosyan, Roberto Henschel, Zhangyang Wang, Shant Navasardyan, and Humphrey Shi. Text2video-zero: Text-to-image diffusion models are zero-shot video generators. In *Proceedings of the IEEE/CVF International Conference on Computer Vision*, pages 15954–15964, 2023.
- [17] Edward J Hu, Yelong Shen, Phillip Wallis, Zeyuan Allen-Zhu, Yuanzhi Li, Shean Wang, Lu Wang, Weizhu Chen, et al. Lora: Low-rank adaptation of large language models. *ICLR*, 1(2):3, 2022.
- [18] Xiang Wang, Shiwei Zhang, Han Zhang, Yu Liu, Yingya Zhang, Changxin Gao, and Nong Sang. Videolcm: Video latent consistency model. *arXiv preprint arXiv:2312.09109*, 2023.
- [19] Yang Song, Prafulla Dhariwal, Mark Chen, and Ilya Sutskever. Consistency models. 2023.
- [20] Simian Luo, Yiqin Tan, Longbo Huang, Jian Li, and Hang Zhao. Latent consistency models: Synthesizing high-resolution images with few-step inference. *arXiv preprint arXiv:2310.04378*, 2023.
- [21] Jiaming Song, Chenlin Meng, and Stefano Ermon. Denoising diffusion implicit models. *arXiv preprint arXiv:2010.02502*, 2020.
- [22] Jonathan Ho, Ajay Jain, and Pieter Abbeel. Denoising diffusion probabilistic models. *Advances in neural information processing systems*, 33:6840–6851, 2020.
- [23] Yang Song, Jascha Sohl-Dickstein, Diederik P Kingma, Abhishek Kumar, Stefano Ermon, and Ben Poole. Score-based generative modeling through stochastic differential equations. *arXiv preprint arXiv:2011.13456*, 2020.
- [24] Alex Nichol, Prafulla Dhariwal, Aditya Ramesh, Pranav Shyam, Pamela Mishkin, Bob McGrew, Ilya Sutskever, and Mark Chen. Glide: Towards photorealistic image generation and editing with text-guided diffusion models. *arXiv preprint arXiv:2112.10741*, 2021.
- [25] Black Forest Labs. Flux.1-schnell, 2024. Accessed: 2024-08-17.

- [26] Patrick Esser, Sumith Kulal, Andreas Blattmann, Rahim Entezari, Jonas Müller, Harry Saini, Yam Levi, Dominik Lorenz, Axel Sauer, Frederic Boesel, et al. Scaling rectified flow transformers for high-resolution image synthesis. In *Forty-first International Conference on Machine Learning*, 2024.
- [27] Xinchen Zhang, Ling Yang, Guohao Li, Yaqi Cai, Jiake Xie, Yong Tang, Yujiu Yang, Mengdi Wang, and Bin Cui. Itercomp: Iterative composition-aware feedback learning from model gallery for text-to-image generation. *arXiv preprint arXiv:2410.07171*, 2024.
- [28] Robin Rombach, Andreas Blattmann, Dominik Lorenz, Patrick Esser, and Björn Ommer. High-resolution image synthesis with latent diffusion models. In *Proceedings of the IEEE/CVF conference on computer vision and pattern recognition*, pages 10684–10695, 2022.
- [29] Chitwan Saharia, William Chan, Saurabh Saxena, Lala Li, Jay Whang, Emily L Denton, Kamyar Ghasemipour, Raphael Gontijo Lopes, Burcu Karagol Ayan, Tim Salimans, et al. Photorealistic text-to-image diffusion models with deep language understanding. *Advances in neural information processing systems*, 35:36479–36494, 2022.
- [30] James Betker, Gabriel Goh, Li Jing, Tim Brooks, Jianfeng Wang, Linjie Li, Long Ouyang, Juntang Zhuang, Joyce Lee, Yufei Guo, et al. Improving image generation with better captions. *Computer Science*. <https://cdn.openai.com/papers/dall-e-3.pdf>, 2(3):8, 2023.
- [31] Dustin Podell, Zion English, Kyle Lacey, Andreas Blattmann, Tim Dockhorn, Jonas Müller, Joe Penna, and Robin Rombach. Sdxl: Improving latent diffusion models for high-resolution image synthesis. *arXiv preprint arXiv:2307.01952*, 2023.
- [32] Runway Research. Introducing gen-3 alpha: A new frontier for video generation, 2024. Runway Gen-3 technical report.
- [33] Ozgun Ciccek, Ahmed Abdulkadir, Soeren S Lienkamp, Thomas Brox, and Olaf Ronneberger. 3d u-net: learning dense volumetric segmentation from sparse annotation. In *Medical Image Computing and Computer-Assisted Intervention–MICCAI 2016: 19th International Conference, Athens, Greece, October 17–21, 2016, Proceedings, Part II 19*, pages 424–432. Springer, 2016.
- [34] Jonathan Ho, William Chan, Chitwan Saharia, Jay Whang, Ruiqi Gao, Alexey Gritsenko, Diederik P. Kingma, Ben Poole, Mohammad Norouzi, David J. Fleet, and Tim Salimans. Imagen video: High definition video generation with diffusion models, 2022.
- [35] Uriel Singer, Adam Polyak, Thomas Hayes, Xi Yin, Jie An, Songyang Zhang, Qiyuan Hu, Harry Yang, Oron Ashual, Oran Gafni, et al. Make-a-video: Text-to-video generation without text-video data. *arXiv preprint arXiv:2209.14792*, 2022.
- [36] Yingqing He, Tianyu Yang, Yong Zhang, Ying Shan, and Qifeng Chen. Latent video diffusion models for high-fidelity long video generation. *arXiv preprint arXiv:2211.13221*, 2022.
- [37] Andreas Blattmann, Robin Rombach, Huan Ling, Tim Dockhorn, Seung Wook Kim, Sanja Fidler, and Karsten Kreis. Align your latents: High-resolution video synthesis with latent diffusion models. In *Proceedings of the IEEE/CVF conference on computer vision and pattern recognition*, pages 22563–22575, 2023.
- [38] Daquan Zhou, Weimin Wang, Hanshu Yan, Weiwei Lv, Yizhe Zhu, and Jiashi Feng. Magicvideo: Efficient video generation with latent diffusion models. *arXiv preprint arXiv:2211.11018*, 2022.
- [39] Max Bain, Arsha Nagrani, Gül Varol, and Andrew Zisserman. Frozen in time: A joint video and image encoder for end-to-end retrieval. In *Proceedings of the IEEE/CVF international conference on computer vision*, pages 1728–1738, 2021.
- [40] Hongwei Xue, Tiankai Hang, Yanhong Zeng, Yuchong Sun, Bei Liu, Huan Yang, Jianlong Fu, and Baining Guo. Advancing high-resolution video-language representation with large-scale video transcriptions. In *Proceedings of the IEEE/CVF Conference on Computer Vision and Pattern Recognition*, pages 5036–5045, 2022.

- [41] Yuwei Guo, Ceyuan Yang, Anyi Rao, Zhengyang Liang, Yaohui Wang, Yu Qiao, Maneesh Agrawala, Dahua Lin, and Bo Dai. Animatediff: Animate your personalized text-to-image diffusion models without specific tuning. *arXiv preprint arXiv:2307.04725*, 2023.
- [42] Haoxin Chen, Yong Zhang, Xiaodong Cun, Menghan Xia, Xintao Wang, Chao Weng, and Ying Shan. Videocrafter2: Overcoming data limitations for high-quality video diffusion models. In *Proceedings of the IEEE/CVF Conference on Computer Vision and Pattern Recognition*, pages 7310–7320, 2024.
- [43] Jay Zhangjie Wu, Yixiao Ge, Xintao Wang, Stan Weixian Lei, Yuchao Gu, Yufei Shi, Wynne Hsu, Ying Shan, Xiaohu Qie, and Mike Zheng Shou. Tune-a-video: One-shot tuning of image diffusion models for text-to-video generation. In *Proceedings of the IEEE/CVF International Conference on Computer Vision*, pages 7623–7633, 2023.
- [44] Lvmin Zhang, Anyi Rao, and Maneesh Agrawala. Adding conditional control to text-to-image diffusion models. In *Proceedings of the IEEE/CVF international conference on computer vision*, pages 3836–3847, 2023.
- [45] Xinyu Zhang, Zicheng Duan, Dong Gong, and Lingqiao Liu. Training-free motion-guided video generation with enhanced temporal consistency using motion consistency loss. *arXiv preprint arXiv:2501.07563*, 2025.
- [46] Jonathan Ho and Tim Salimans. Classifier-free diffusion guidance. *arXiv preprint arXiv:2207.12598*, 2022.
- [47] Jiwen Yu, Yinhuai Wang, Chen Zhao, Bernard Ghanem, and Jian Zhang. Freedom: Training-free energy-guided conditional diffusion model. In *Proceedings of the IEEE/CVF International Conference on Computer Vision*, pages 23174–23184, 2023.
- [48] Haotian Ye, Haowei Lin, Jiaqi Han, Minkai Xu, Sheng Liu, Yitao Liang, Jianzhu Ma, James Zou, and Stefano Ermon. Tfg: Unified training-free guidance for diffusion models. *arXiv preprint arXiv:2409.15761*, 2024.
- [49] Fu-Yun Wang, Zhaoyang Huang, Weikang Bian, Xiaoyu Shi, Keqiang Sun, Guanglu Song, Yu Liu, and Hongsheng Li. Animatelem: Computation-efficient personalized style video generation without personalized video data. In *SIGGRAPH Asia 2024 Technical Communications*, pages 1–5. 2024.
- [50] Geoffrey Hinton, Oriol Vinyals, and Jeff Dean. Distilling the knowledge in a neural network. *arXiv preprint arXiv:1503.02531*, 2015.
- [51] Haonan Qiu, Zhaoxi Chen, Zhouxia Wang, Yingqing He, Menghan Xia, and Ziwei Liu. Freetrajectory: Tuning-free trajectory control in video diffusion models. *arXiv preprint arXiv:2406.16863*, 2024.
- [52] Haonan Qiu, Menghan Xia, Yong Zhang, Yingqing He, Xintao Wang, Ying Shan, and Ziwei Liu. Freenoise: Tuning-free longer video diffusion via noise rescheduling. *arXiv preprint arXiv:2310.15169*, 2023.
- [53] Jordi Pont-Tuset, Federico Perazzi, Sergi Caelles, Pablo Arbeláez, Alex Sorkine-Hornung, and Luc Van Gool. The 2017 davis challenge on video object segmentation. *arXiv preprint arXiv:1704.00675*, 2017.
- [54] Max Bain, Arsha Nagrani, Gül Varol, and Andrew Zisserman. Frozen in time: A joint video and image encoder for end-to-end retrieval. In *Proceedings of the IEEE/CVF international conference on computer vision*, pages 1728–1738, 2021.
- [55] Alec Radford, Jong Wook Kim, Chris Hallacy, Aditya Ramesh, Gabriel Goh, Sandhini Agarwal, Girish Sastry, Amanda Askell, Pamela Mishkin, Jack Clark, et al. Learning transferable visual models from natural language supervision. In *International conference on machine learning*, pages 8748–8763. PmLR, 2021.

- [56] Nikita Karaev, Ignacio Rocco, Benjamin Graham, Natalia Neverova, Andrea Vedaldi, and Christian Rupprecht. Cotracker: It is better to track together. In *European Conference on Computer Vision*, pages 18–35. Springer, 2024.
- [57] Naresh Babu Bynagari. Gans trained by a two time-scale update rule converge to a local nash equilibrium. *Asian J. Appl. Sci. Eng*, 8(1):25–34, 2019.

Training-Free Motion Customization for Distilled Video Generators with Adaptive Test-Time Distillation

Supplementary Material

A More Details of the Method

A.1 Pseudo Code

To provide a clearer understanding of our proposed test-time distillation framework, we present the detailed pseudo code in Algorithm 1. The algorithm describes the overall inference procedure for motion-customized video generation using a distilled student model guided by a fine-grained teacher model. Specifically, it consists of three main stages at each denoising step: (1) latent customized prediction by the distilled student model, (2) conditional activation of teacher guidance based on the average motion loss, and (3) latent refinement via score distillation. The algorithm also incorporates an adaptive acceleration strategy, which dynamically determines when and how intensively teacher supervision should be applied, ensuring an optimal trade-off between efficiency and motion fidelity.

B Additional Experimental Details and Results

B.1 Baseline Description

- ControlVideo [12] injects HED boundaries as the control signals and finetunes key-frame and temporal attention to enable full cross-frame interaction with a pre-trained diffusion model, ensuring high-quality and consistent text-driven video editing.
- Control-A-Video [13] incorporates first-frame condition and uses reward feedback to enhance visual quality and motion consistency.
- MotionDirector [9] achieves motion customization by injecting dual-path LoRAs into a pre-trained text-to-video diffusion model, where spatial LoRAs capture appearance and temporal LoRAs model motion, effectively disentangling the two factors.
- MotionInversion [10] learns explicit motion embeddings from a reference video, which are injected into the temporal modules of the text-to-video diffusion model to guide motion generation while removing appearance bias.
- MotionClone [14] extracts motion priors from the temporal attention matrix of a reference video and constructs an energy function to guide the sampling process of the pretrained text-to-video model.
- DMT [15] obtains space-time features from intermediate layer activations of the diffusion model and introduces a handcrafted loss to guide motion customization during inference.

B.2 Noise Initialization

Similar to previous works [51, 52], noise initialization is crucial for the final generated results. To this end, we detail the initialization strategies employed by various baselines as well as our method in the experiment. ControlVideo [57], Control-A-Video [13] and MotionClone [14] adopt random noise initialization. DMT [15] extracts low-frequency components by downsampling the random noise and replaces them with those from the inversion noise of the reference video. MotionDirector [9] and MotionInversion [10] linearly blend the random noise and inverted reference noise, modulated by a scaling factor set to 0.5 in experiments. We follow the blending strategy by setting the factor as 0.01, enabling better motion preservation while maintaining generation diversity.

B.3 Additional Ablation Study Results

The hyper-parameters in our method are determined via grid search. Here, we present additional ablation study results.

Table 4: Ablation study on the effect of teacher guidance strength λ .

λ	Temporal Consistency (\uparrow)	Text Alignment (\uparrow)	Motion Fidelity (\uparrow)	FID (\downarrow)
0.1	0.975	0.341	0.924	332.23
0.3	0.977	0.344	0.936	323.91
0.5	0.976	0.359	0.930	320.10

Table 5: Ablation study on the effect of motion guidance strength η .

η	Temporal Consistency (\uparrow)	Text Alignment (\uparrow)	Motion Fidelity (\uparrow)	FID (\downarrow)
500	0.978	0.350	0.929	323.91
1000	0.973	0.341	0.935	327.77
2000	0.966	0.338	0.940	325.17

Effect of Teacher Guidance Strength λ . Tab. 4 shows how varying the teacher guidance strength λ influences the generated video quality. We observe that $\lambda = 0.3$ offers the best overall trade-off across three metrics.

Effect of Motion Guidance Strength η . As shown in Tab. 5, motion guidance strength η controls how strictly the model follows the reference motion. Increasing η improves motion fidelity but reduce textual alignment or introduce temporal artifacts when overly strong.

Effect of Blend Scaling Factor k . We blend the random noise and inverted reference noise during initialization. Tab. 6 reports ablation study results for camera motion customization, where a balanced blend factor $k = 0.01$ improves spatial coherence and textual alignment. Tab. 7 provides results for hybrid and object motion customization.

B.4 Additional Qualitative Results

We provide more visual results for qualitative evaluation.

Diversity. As shown in Fig.8 and Fig.9, MotionEcho demonstrates strong adaptability across diverse scenarios. For object motion customization, our method successfully generates fine-grained motion for various subjects, such as a duck swimming in a river, a tiger raising its head, and a monkey turning in the forest, preserving semantic consistency while reflecting distinct object behaviors. For camera motion customization, we exhibit faithful reproduction of different camera trajectories including clockwise rotation, zoom out, pan down, pan up, capturing dynamic environmental changes (*e.g.*, fireworks near a tower, a snowy field, or a forest scene). These results validate the robustness of our approach under a wide spectrum of motion types and visual contexts.

Generalization. To further verify the flexibility and effectiveness of our method, we evaluate its generalization capability in two aspects. First, *in terms of motion customization strategies*, our method is integrated with both MotionClone [14] and MotionDirector [9], leveraging the T2V-Turbo-V2 backbone [1]. As shown in Fig. 10, the visual results demonstrate that our framework maintains consistent performance when paired with different motion guidance modules, confirming its adaptability and robustness. Second, *in terms of baseline models*, we integrate our framework with different combinations of student and teacher models (*e.g.*, AnimateDiff-Lightning [2] and AnimateDiff [41]). As shown in Fig.11, our method still generate stable and high-quality motion-customized videos.

Alignment. Fig. 12 qualitatively illustrates the effectiveness of our method in aligning motion representations with the reference video, exhibiting strong spatial and temporal consistency.

Comparison. In Fig. 4 and Fig. 5 of the main paper, we provide some exemplar cases of comparing our methods with the other motion customization models including training-based methods (*e.g.*, ControlVideo [57], Control-A-Video [13], MotionDirector [9], MotionInverison [10]) and training-free methods (*e.g.*, MotionClone [14], DMT [15]). Here, we provide a more comprehensive comparison

Table 6: Ablation study on the effect of blend scaling factor k in noise initialization for camera motion customization.

k	Temporal Consistency (\uparrow)	Text Alignment (\uparrow)	Motion Fidelity (\uparrow)	FID (\downarrow)
0.01	0.978	0.333	0.963	315.69
0.05	0.975	0.328	0.974	314.24
0.1	0.967	0.315	0.973	324.87

Table 7: Ablation study on the effect of blend scaling factor k in noise initialization for hybrid and object motion customization.

k	Temporal Consistency (\uparrow)	Text Alignment (\uparrow)	Motion Fidelity (\uparrow)	FID (\downarrow)
0.1	0.972	0.352	0.912	334.06
0.3	0.972	0.351	0.923	329.28
0.5	0.967	0.347	0.910	339.86

with more examples of generated videos, covering camera motion (Fig. 13), hybrid motion (Fig. 14, Fig. 15, Fig. 16) and object motion (Fig. 17, Fig. 18). It is observed that our method achieves superior motion fidelity and temporal coherence under the 16-step setting. Remarkably, even when the number of steps is reduced to 8 or 4—significantly lowering inference time—our method still achieves competitive visual quality, highlighting its efficiency and robustness for fast and high-quality motion customization.

B.5 Additional Details on Human Evaluation

We conduct a user study to assess the perceptual quality of motion-customized videos generated by MotionEcho. Specifically, the study is implemented via an online survey form, which is divided into multiple sections. Each section corresponds to a specific test case consisting of a reference video, a given prompt and generated videos by our method and baselines. Within each section, investigators are required to answer four questions (Q1–Q4), corresponding to Fig. 19, Fig. 20, Fig. 21 and Fig. 22. In addition, investigators are recruited through an online platform, ensuring their anonymity. Each investigator is required to have at least a bachelor’s degree and their privacy and identity are kept confidential throughout the entire process. Finally, the collected responses are aggregated to perform comparative analysis across different methods in terms of user-perceived quality.

C Ethical and Social Impacts

The development of MotionEcho, a training-free test-time distillation framework for motion customization, is a double-edged sword. On one hand, our method enables efficient and flexible motion transfer without any training, which opens up new possibilities for creative industries, education, and accessibility by allowing users to generate personalized videos with minimal resources.

On the other hand, the powerful capabilities of MotionEcho raise important concerns regarding potential misuse. Our method relies on the pre-trained text-to-video diffusion models, which are trained on large-scale datasets sourced from the internet or generated content. These datasets may contain biased, inappropriate, unsafe or copyrighted material, potentially leading to the inadvertent propagation of societal stereotypes or unauthorized replication of proprietary content. Additionally, the ability to generate highly realistic motion-aligned videos with minimal effort increases the risk of misuse, such as fabricating misleading media or deepfakes. To mitigate these risks, we advocate for the implementation of ethical safeguards, including automated content filtering, watermark-based provenance tracking, and clearly defined usage policies that prioritize transparency, accountability, and user consent.

To promote transparency in AI-generated content and foster further research in video generation, the source code will be made publicly available upon acceptance of the paper. We hope that open access to this technology will catalyze collaborative efforts toward safer and more inclusive generative systems.

Algorithm 1 Adaptive Test-time Distillation for Motion Customization

- 1: **Input:** Distilled video diffusion model ϵ_ψ , Fine-grained teacher model ϵ_θ , Reference latent z^{ref} , Text prompt c , Unconditional prompt ϕ , Teacher guidance schedule ratio τ , Blend scaling factor k , Motion guidance strength η , Teacher guidance strength λ , Motion thresholds δ_1, δ_2 , Window size W , Teacher’s max inner denoising steps N_{max} , Total student sampling steps N_s , Total teacher sampling steps N_t .
 - 2: **Output:** Final denoised latent z_0^ψ .
 - 3:
 - 4: $z_T^{\text{ref}}, z_{t_\alpha}^{\text{ref}} = \text{DDIM Inversion}(z^{\text{ref}})$
 - 5: $\epsilon_T \sim \mathcal{N}(0, \mathbf{I})$
 - 6: Initialize blended noise: $z_T^\psi = \sqrt{k}z_T^{\text{ref}} + \sqrt{1-k}\epsilon_T$
 - 7: Set $\Delta t_s = T/N_s, \Delta t_t = T/N_t$
 - 8: **for** $t = T$ **to** Δt_s **by** $-\Delta t_s$ **do**
 - 9: **Stage 1. Student Customization**
 - 10: $\tilde{\epsilon}_\psi(z_t^\psi, c, t) = (1 + \omega_\psi)\epsilon_\psi(z_t^\psi, c, t) - \omega_\psi\epsilon_\psi(z_t^\psi, \phi, t)$
 - 11: $\hat{z}_{0 \leftarrow t}^\psi = \frac{z_t^\psi - \sqrt{1 - \bar{\alpha}_t}\tilde{\epsilon}_\psi(z_t^\psi, c, t)}{\sqrt{\bar{\alpha}_t}}$ \triangleright Without motion guidance
 - 12: $\hat{\epsilon}_\psi(z_t^\psi, c, t) = (1 + \omega_\psi)\epsilon_\psi(z_t^\psi, c, t) - \omega_\psi\epsilon_\psi(z_t^\psi, \phi, t) - \eta \cdot \nabla_{z_t^\psi} \mathcal{G}^m(z_t^\psi, z_{t_\alpha}^{\text{ref}}, t)$
 - 13: $\hat{z}_{0 \leftarrow t}^\psi = \frac{z_t^\psi - \sqrt{1 - \bar{\alpha}_t}\hat{\epsilon}_\psi(z_t^\psi, c, t)}{\sqrt{\bar{\alpha}_t}}$ \triangleright With motion guidance
 - 14: **Stage 2. Adaptive Teacher Guidance**
 - 15: **if** $t > \tau \cdot T$ **then**
 - 16: $\text{avg}_{\mathcal{G}}^\psi(t) = \frac{1}{W} \sum_{j=0}^{W-1} \mathcal{G}^m(z_{t+j \cdot \Delta t_s}^\psi, z_{t_\alpha}^{\text{ref}}, t + j \cdot \Delta t_s)$ \triangleright Moving average motion loss
 - 17: **if** $\text{avg}_{\mathcal{G}}^\psi(t) > \delta_1$ **then**
 - 18: Select inner teacher step $s \in (t, t - \Delta t_s)$
 - 19: $z_s^\theta = \sqrt{\bar{\alpha}_s}\tilde{z}_{0 \leftarrow t}^\psi + \sqrt{1 - \bar{\alpha}_s}\epsilon, \epsilon \sim \mathcal{N}(0, I)$ \triangleright Renoise
 - 20: **for** $n = s$ **to** $t - \Delta t_s$ **by** $-\Delta t_t$ **do**
 - 21: $\hat{\epsilon}_\theta(z_n^\theta, c, n) = (1 + \omega_\theta)\epsilon_\theta(z_n^\theta, c, n) - \omega_\theta\epsilon_\theta(z_n^\theta, \phi, n) - \eta \cdot \nabla_{z_n^\theta} \mathcal{G}^m(z_n^\theta, z_{t_\alpha}^{\text{ref}}, n)$
 - 22: $\hat{z}_{0 \leftarrow n}^\theta = \frac{z_n^\theta - \sqrt{1 - \bar{\alpha}_n}\hat{\epsilon}_\theta(z_n^\theta, c, n)}{\sqrt{\bar{\alpha}_n}}$ \triangleright Teacher motion customization
 - 23: **if** $\mathcal{G}^m(z_n^\theta, z_{t_\alpha}^{\text{ref}}, n) < \delta_2$ **or** $\frac{s-n}{\Delta t_t} > N_{\text{max}}$ **then**
 - 24: $z_{t-\Delta t_s}^\theta = \sqrt{\bar{\alpha}_{t-\Delta t_s}}\hat{z}_{0 \leftarrow n}^\theta + \sqrt{1 - \bar{\alpha}_{t-\Delta t_s}}\epsilon, \epsilon \sim \mathcal{N}(0, I)$
 - 25: **else**
 - 26: $z_{n-\Delta t_t}^\theta = \sqrt{\bar{\alpha}_{n-\Delta t_t}}\hat{z}_{0 \leftarrow n}^\theta + \sqrt{1 - \bar{\alpha}_{n-\Delta t_t}}\epsilon, \epsilon \sim \mathcal{N}(0, I)$
 - 27: **end if**
 - 28: **end for**
 - 29: $\hat{z}_{0 \leftarrow t-\Delta t_s}^\theta = \frac{z_{t-\Delta t_s}^\theta - \sqrt{1 - \bar{\alpha}_{t-\Delta t_s}}\hat{\epsilon}_\theta(z_{t-\Delta t_s}^\theta, c, t - \Delta t_s)}{\sqrt{\bar{\alpha}_{t-\Delta t_s}}}$ \triangleright One-step prediction
 - 30: $\hat{z}_{0 \leftarrow t}^{\text{new}} = (1 - \lambda)\hat{z}_{0 \leftarrow t}^\psi + \lambda\hat{z}_{0 \leftarrow t-\Delta t_s}^\theta$
 - 31: **else**
 - 32: $\hat{z}_{0 \leftarrow t}^{\text{new}} = \hat{z}_{0 \leftarrow t}^\psi$
 - 33: **end if**
 - 34: **else**
 - 35: $\hat{z}_{0 \leftarrow t}^{\text{new}} = \hat{z}_{0 \leftarrow t}^\psi$
 - 36: **end if**
 - 37: **Stage 3. Update latent**
 - 38: $z_{t-\Delta t_s}^\psi = \sqrt{\bar{\alpha}_{t-\Delta t_s}}\hat{z}_{0 \leftarrow t}^{\text{new}} + \sqrt{1 - \bar{\alpha}_{t-\Delta t_s}}\epsilon, \epsilon \sim \mathcal{N}(0, I)$
 - 39: **end for**
 - 40: **return** z_0^ψ
-

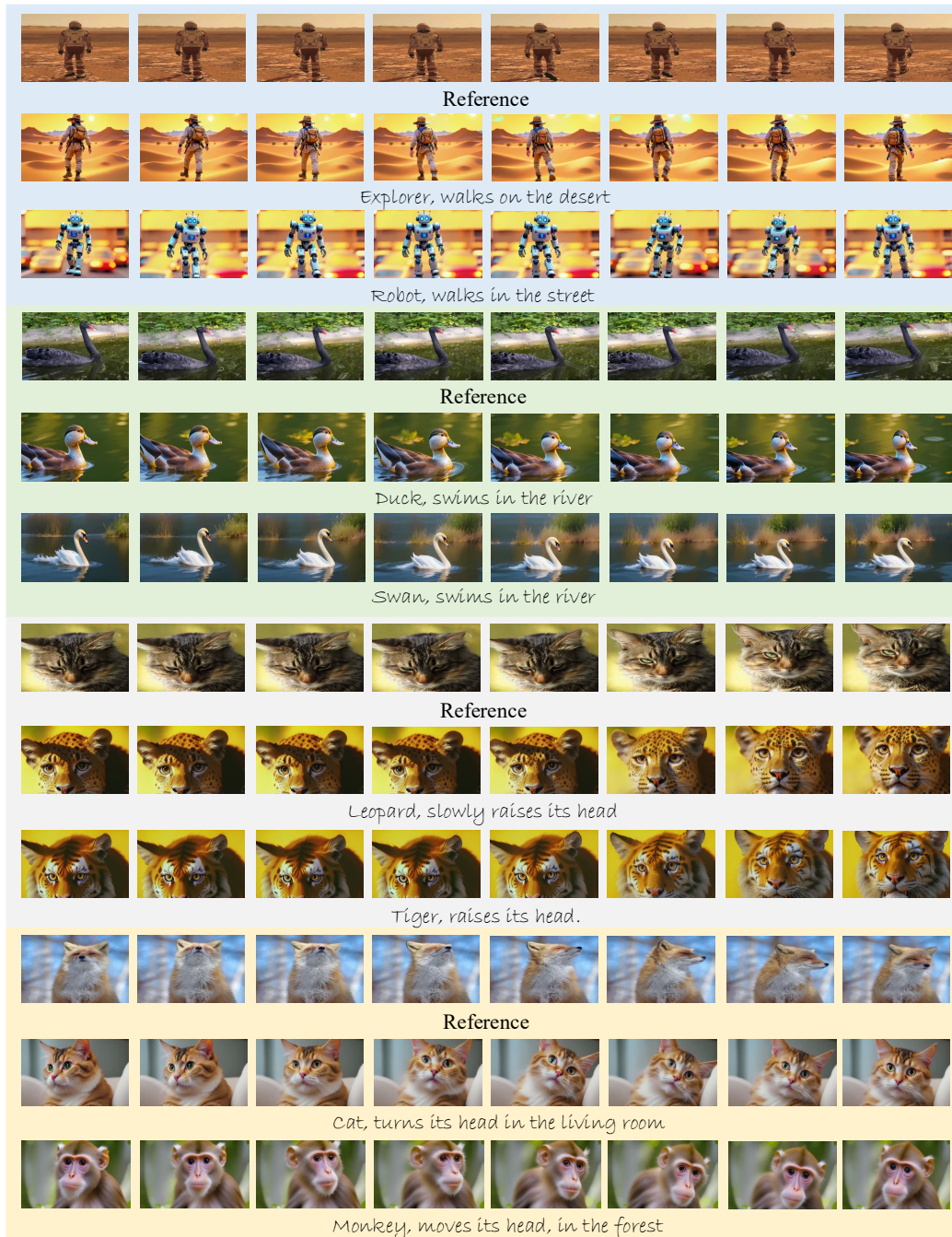


Figure 8: More results of our method (MotionClone+T2V-Turbo-V2) in object motion customization.

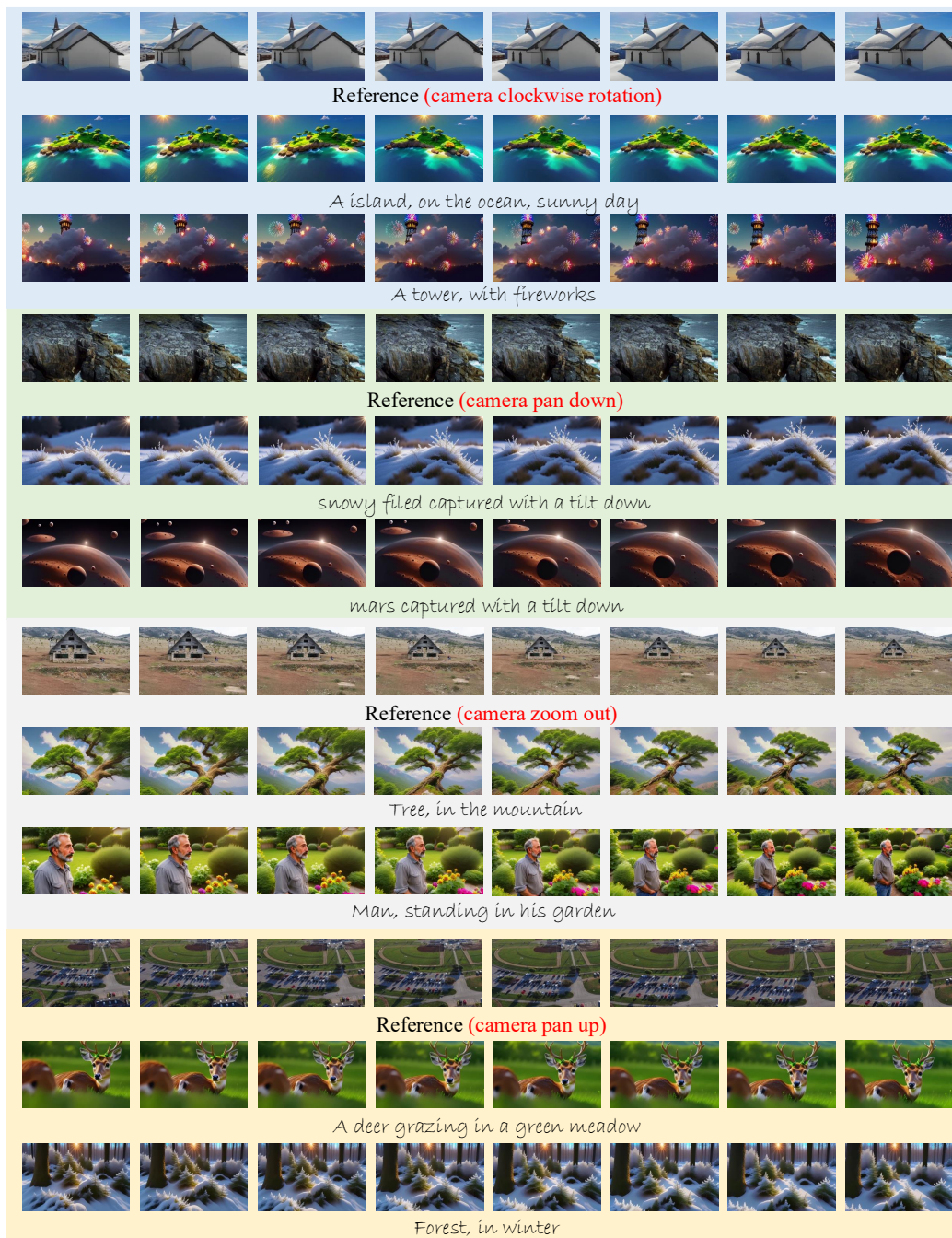


Figure 9: More results of our method (MotionClone+T2V-Turbo-V2) in camera motion customization.

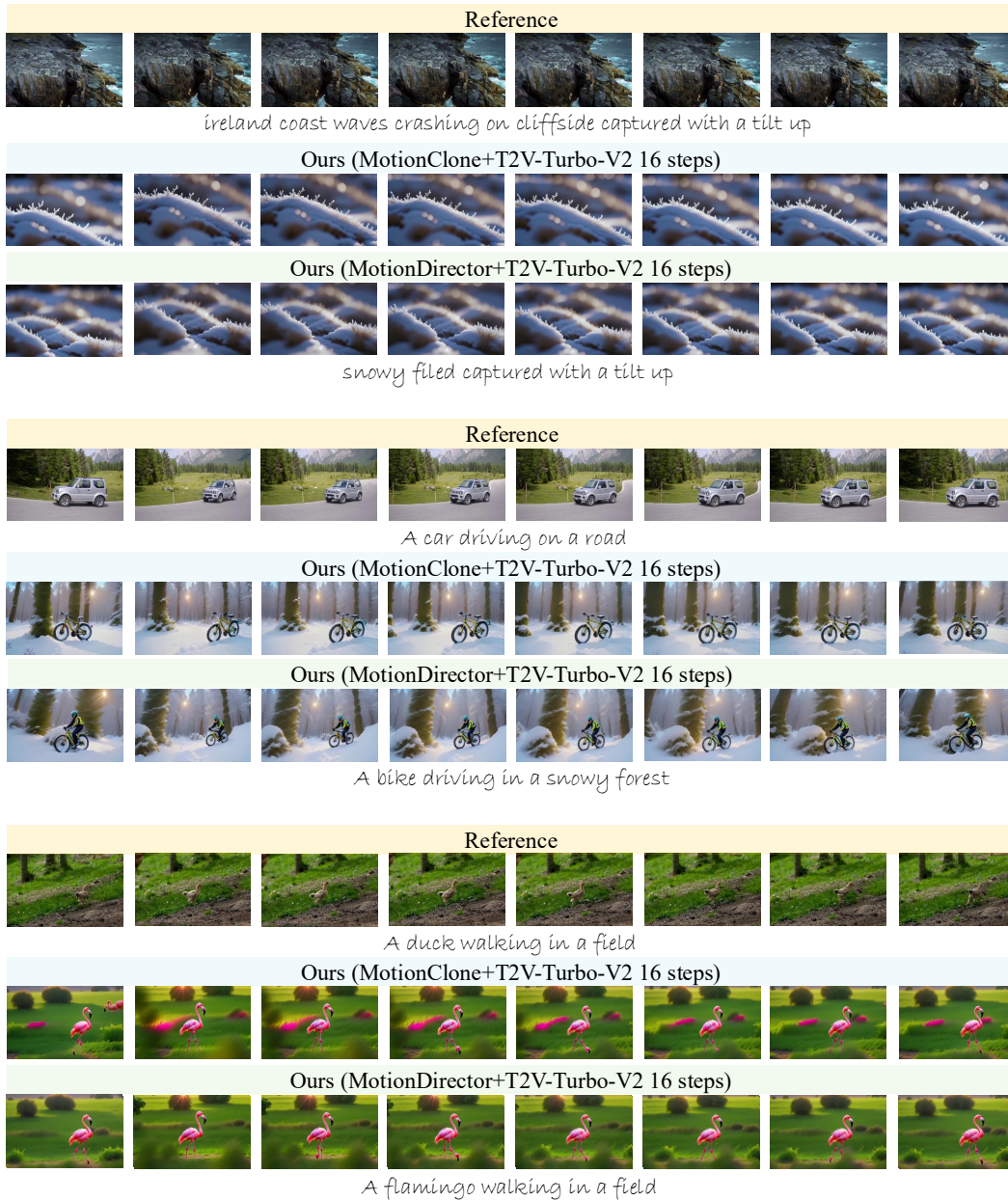


Figure 10: More qualitative results generated by our method under different motion customization strategies.

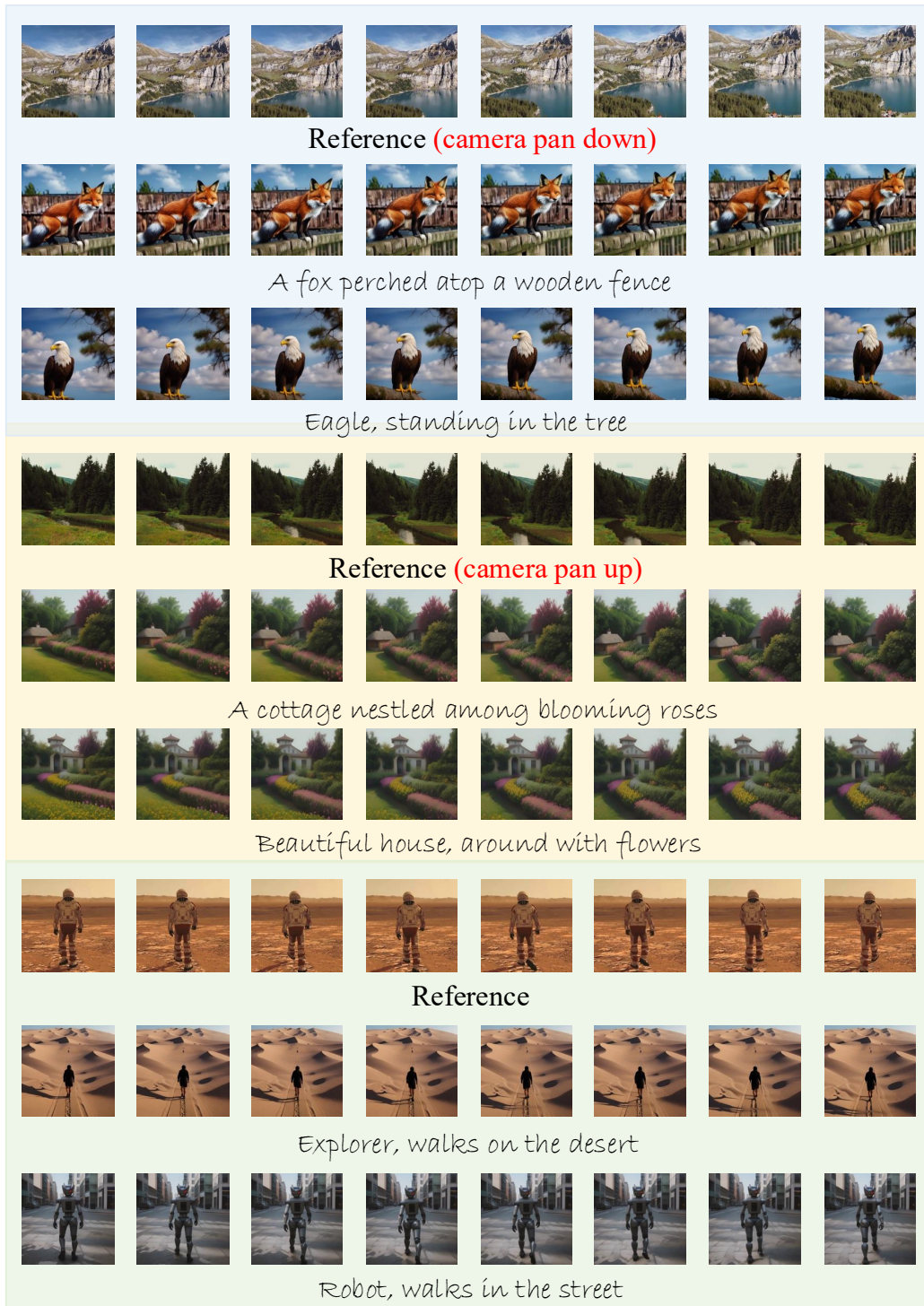


Figure 11: More results of our method (MotionClone+AnimateDiff-Lightning) in camera and object motion customization.

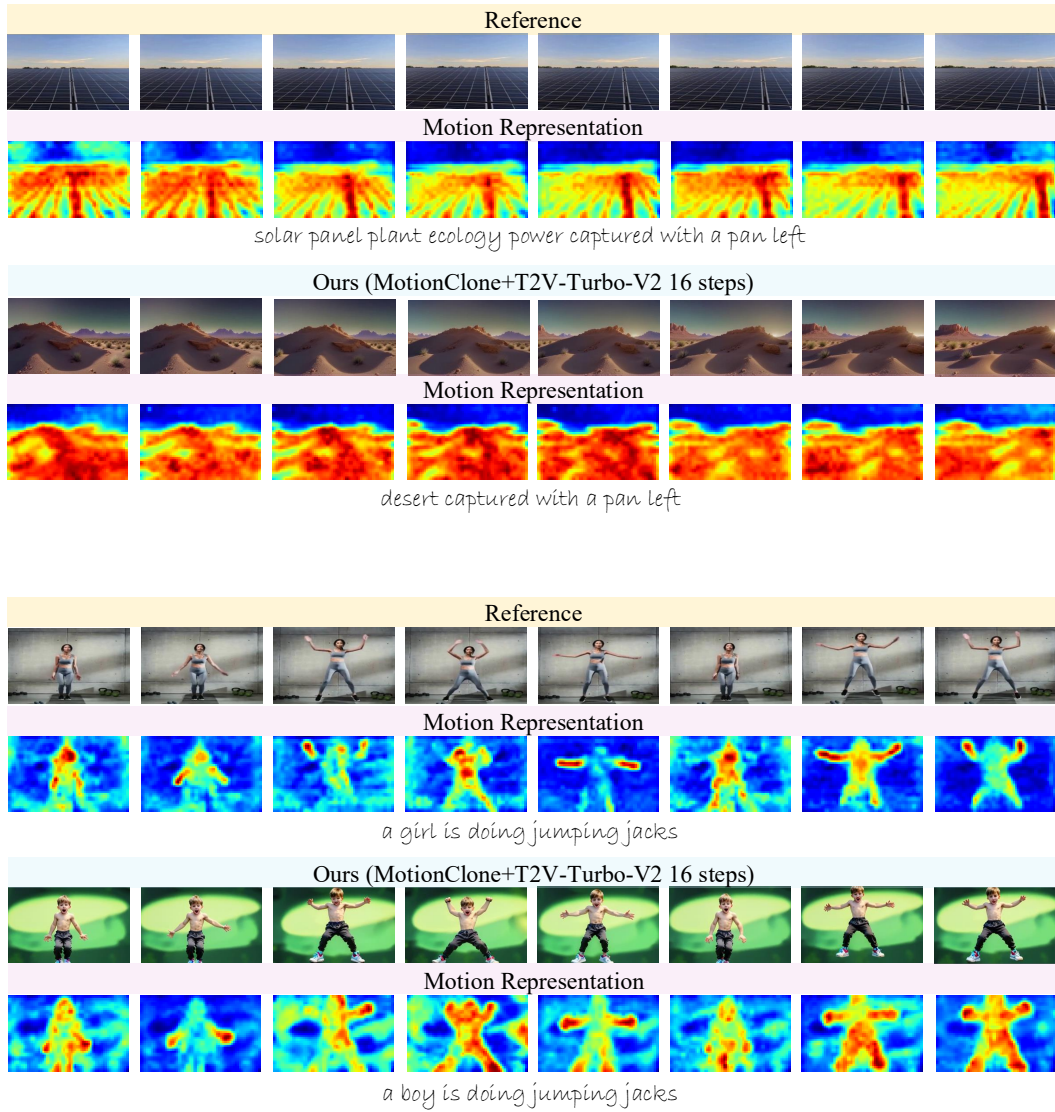


Figure 12: Visualization of motion representation.

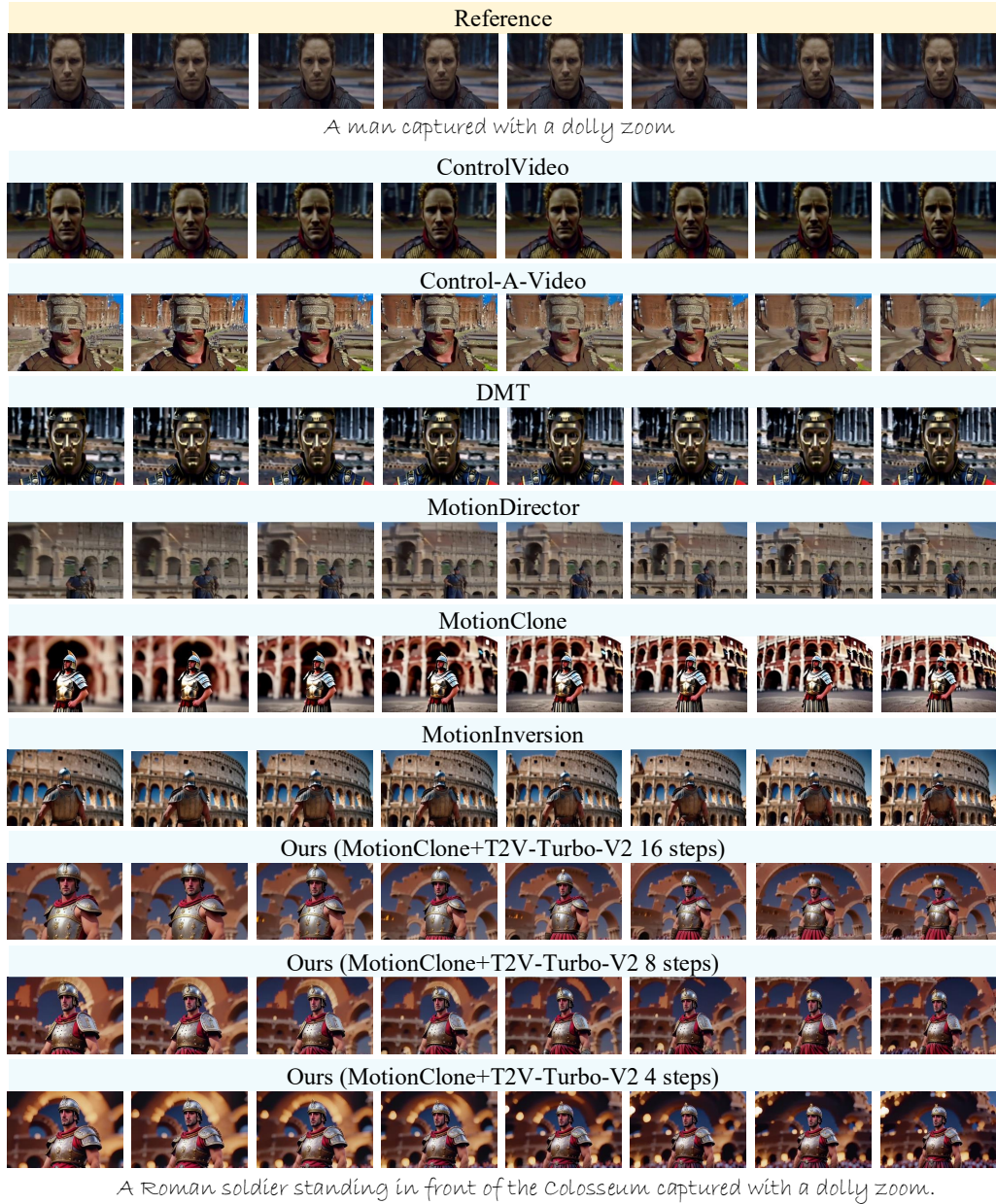


Figure 13: Additional comparison results in camera motion customization.



Figure 14: Additional comparison results in hybrid motion customization.

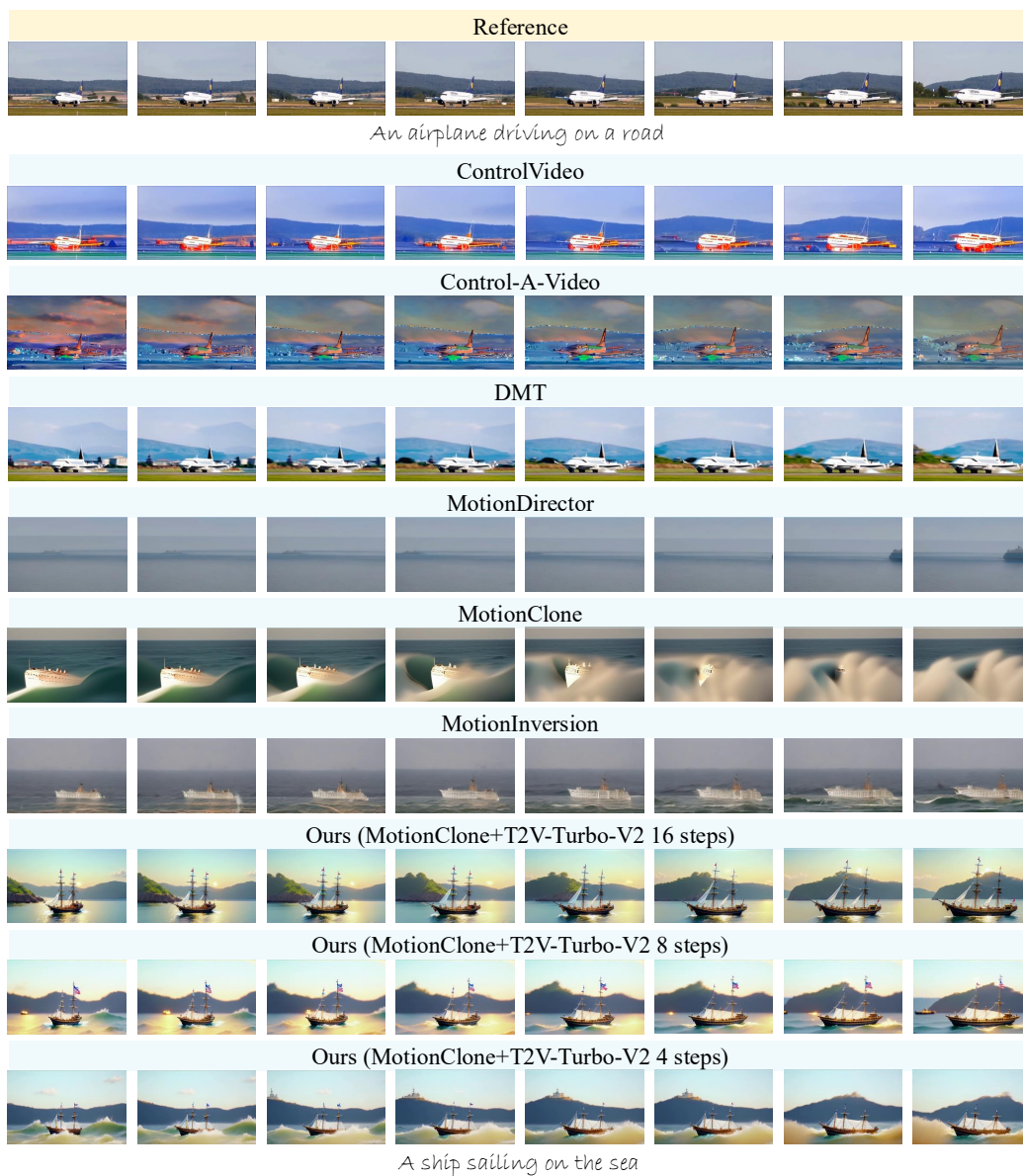


Figure 15: Additional comparison results in hybrid motion customization.



Figure 16: Additional comparison results in hybrid motion customization.

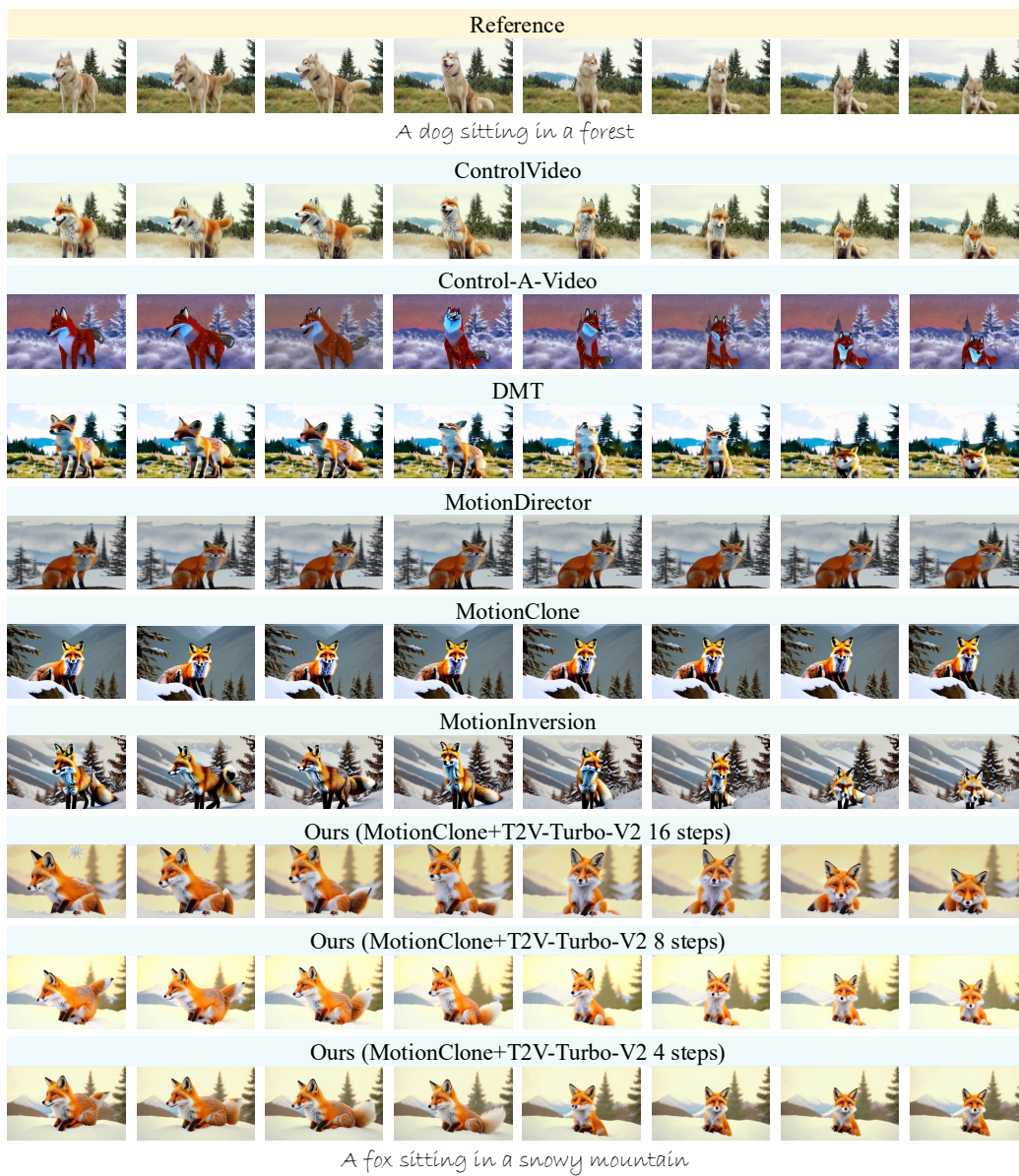


Figure 17: Additional comparison results in object motion customization.

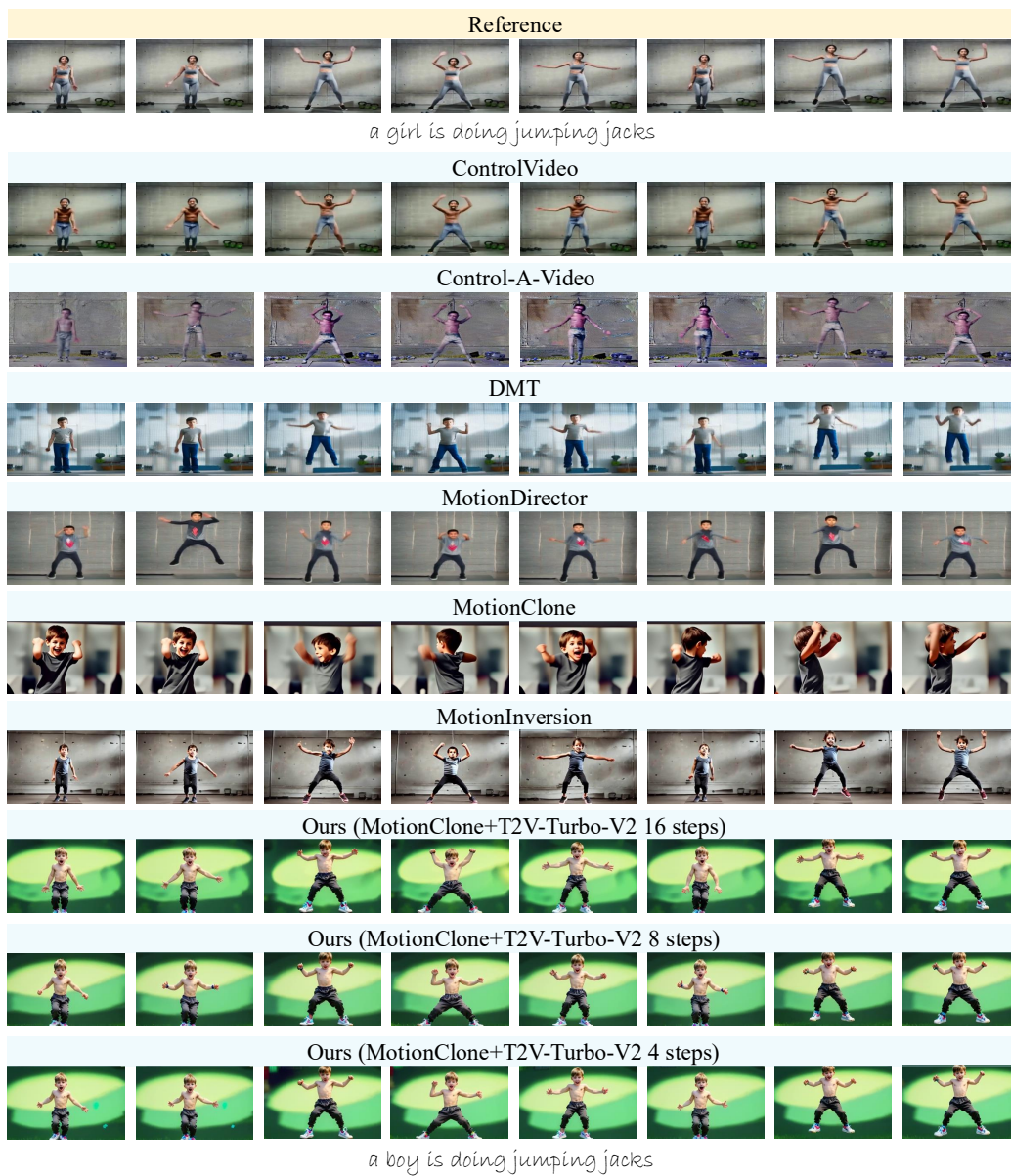


Figure 18: Additional comparison results in object motion customization.

Human Preference Investigation

This task evaluates motion transfer, where the goal is to reproduce the motion patterns from a reference video in a generated result. Given a reference video and its corresponding description, please choose the best one according to the question

- *1. Reference description: A man captured with a dolly zoom



Target description: A firefighter standing in front of a burning forest captured with a dolly zoom.

Question 1: Which video better fits the target text description?

Five options are shown, each with a radio button and a search icon:

- 1: A close-up of a man's face, similar to the reference image.
- 2: A firefighter standing in front of a burning forest, captured with a dolly zoom.
- 3: A close-up of a firefighter's face, wearing a helmet, with a burning forest in the background.
- 4: A firefighter standing in front of a burning forest, captured with a dolly zoom.
- 5: A firefighter standing in front of a burning forest, captured with a dolly zoom.

Figure 19: The screenshot of human preference investigation: Which video better fits the target text description?

*2. Reference description: A man captured with a dolly zoom



Targent description: A firefighter standing in front of a burning forest captured with a dolly zoom.

Question 2: Which video is more consistent across frames?

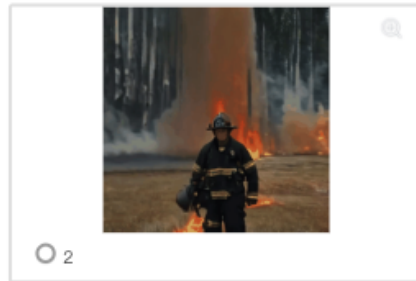


Figure 20: The screenshot of human preference investigation: Which video is more consistent across frames?

*3. Reference description: A man captured with a dolly zoom



Target description: A firefighter standing in front of a burning forest captured with a dolly zoom.

Question 3: Which video better reproduces the motion pattern in the reference?

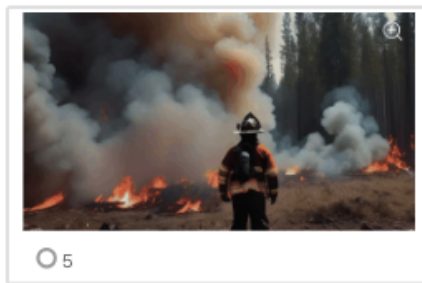
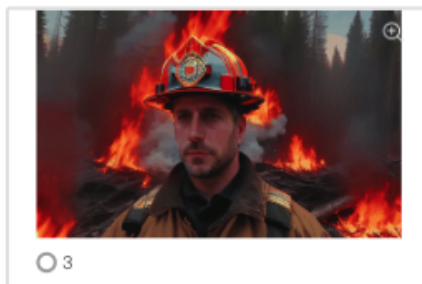
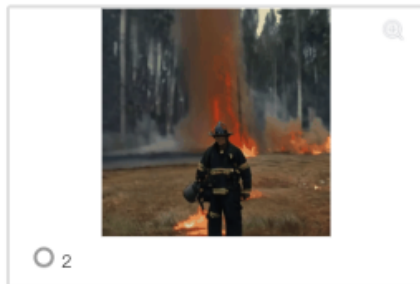


Figure 21: The screenshot of human preference investigation: Which video better reproduces the motion pattern in the reference?

★4. Reference description: A man captured with a dolly zoom



Target description: A firefighter standing in front of a burning forest captured with a dolly zoom.

Question 4: Which video is more visually appealing?

Question 4: Which video is more visually appealing?

1 

2 

3 

4 

5 

Figure 22: The screenshot of human preference investigation: Which video is more visually appealing?